



Upper Triassic–Middle Jurassic resedimented toe-of-slope and hemipelagic basin deposits in the Dinaridic Ophiolite Belt, Zlata Mountain, SW Serbia

János Haas¹ · Divna Jovanović² · Ágnes Görög³ · Milan N. Sudar⁴ · Sándor Józsa⁵ · Péter Ozsvárt⁶ · Pál Pelikán⁷

Received: 24 September 2018 / Accepted: 12 March 2019
© The Author(s) 2019

Abstract

In the Dinaridic Ophiolite Belt, small (m-scale) to large (km-scale) blocks of Middle to Upper Triassic, and Middle to Upper Jurassic, more or less silicified bedded limestone are widely present, both as parts of para-autochthonous successions and as redeposited blocks in ophiolitic mélanges. The studied, approximately 230-m-thick succession in the wider area of Zlata Mountain, is one of the most important para-autochthonous sections in the Serbian part of the Dinaridic Ophiolite Belt. The succession is made up of an alternation of redeposited carbonate toe-of-slope deposits, sand to clay-sized siliciclastic rocks, hemipelagic mudstones and radiolarite–spongiolite basin facies. In the lower part of the sequence, the components of the siliciclastic beds were derived mostly from low- and medium-grade metamorphic rocks. Similar components, together with sand-sized fragments of ophiolitic rocks, were encountered in small amounts in some redeposited carbonate beds. The chronostratigraphic assignment of the succession is based mostly on foraminifers, but age-diagnostic radiolarians and other microfossil groups were also considered. In the lower part of the probably continuous succession, a Norian–Rhaetian assemblage was recognized; a Sinemurian–Pliensbachian assemblage was encountered up-section, whereas the upper part of the succession could be assigned to the Bajocian–Bathonian. Considering the paleogeographic reconstructions and the analogies of age-equivalent sections, the succession records the depositional history of the Bosnian Basin during the Late Triassic to Middle Jurassic period and may contribute to the understanding of the evolution of the Adriatic margin of the Neotethys Ocean in the transition interval from passive to active margin stages.

Keywords Neotethys · Dinaridic Ophiolite Belt · Triassic–Jurassic Serbia · Foraminifers · Radiolarians · Resedimented carbonates · Provenance of siliciclastics

Electronic supplementary material The online version of this article (<https://doi.org/10.1007/s10347-019-0566-3>) contains supplementary material, which is available to authorized users.

✉ János Haas
haas@caesar.elte.hu

- ¹ Eötvös Loránd University, Pázmány Péter sétány 1/C, 1117 Budapest, Hungary
- ² Geological Survey of Serbia, Rovinjska 12, 11000 Belgrade, Serbia
- ³ Department of Palaeontology, Eötvös Loránd University, Pázmány Péter sétány 1/C, 1117 Budapest, Hungary
- ⁴ Serbian Academy of Sciences and Arts, Knez Mihaila 35, 11000 Belgrade, Serbia

Introduction

The Dinaridic ophiolite belt (DOB) (Dimitrijević 1997; Karamata et al. 2000; Dimitrijević et al. 2003; Karamata 2006) with the Dinaridic Ophiolite Nappe on top of the nappe stack

- ⁵ Department of Petrology and Geochemistry, Eötvös Loránd University, Pázmány Péter sétány 1/C, 1117 Budapest, Hungary
- ⁶ MTA-MTM-ELTE, Research Group for Paleontology, PO Box 137, 1431 Budapest, Hungary
- ⁷ Mining and Geological Survey of Hungary, Columbus u.17-23, 1154 Budapest, Hungary

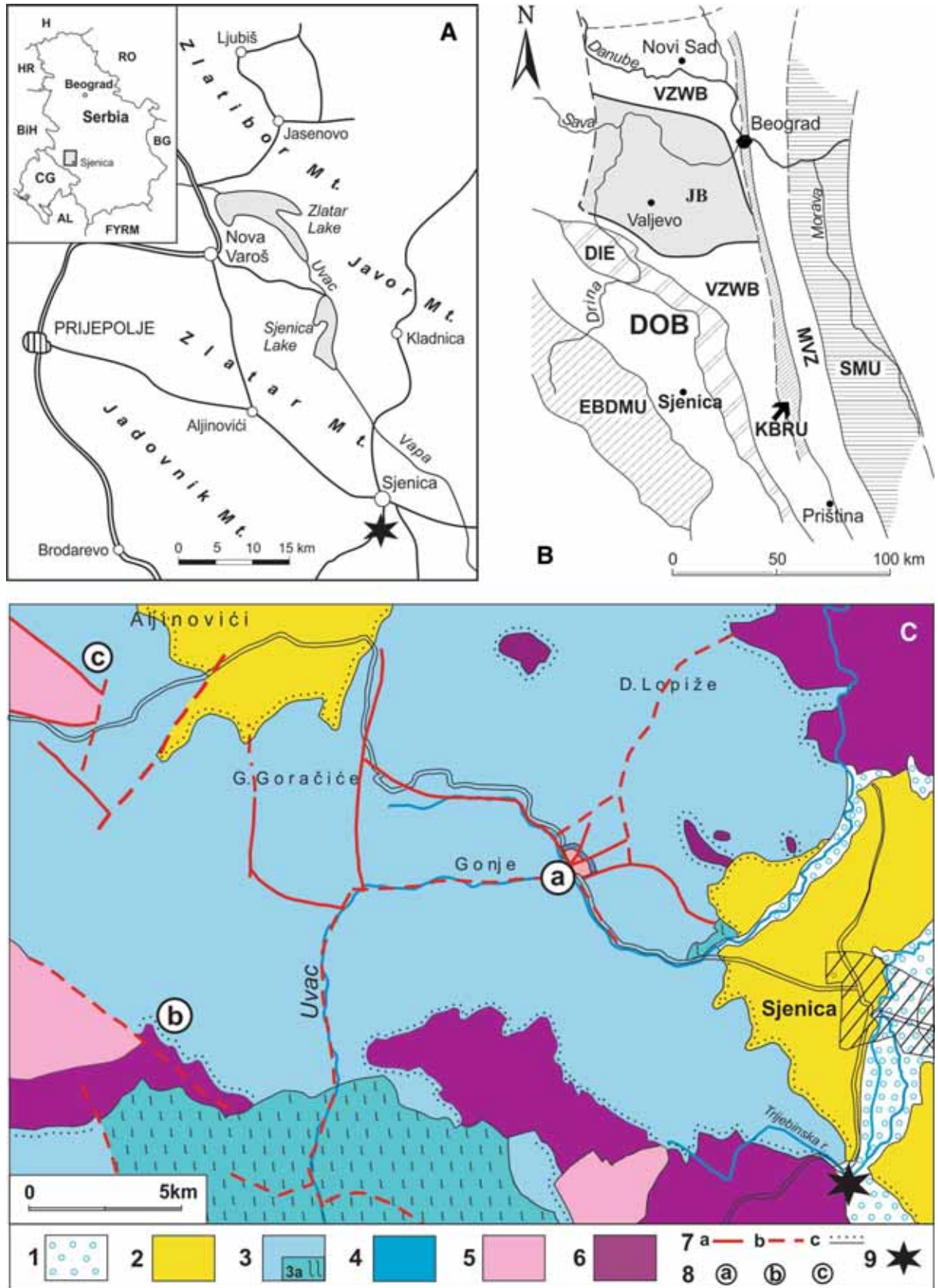


Fig. 1 Locations of the Trijebinska Reka section and geology of the Sjenica area (SW Serbia, the Dinaridic Ophiolite Belt). **a** Geographic position of the Trijebinska Reka section (*black asterisk*) in the south-eastern part of Zlata Mt. **b** Terranes of a part of the Balkan Peninsula (Karamata 2006; Karamata et al. 2000; Gawlick et al. 2017): *SMU* Serbian-Macedonian Unit, *MVZ* Main Vardar Zone, *KBRU* Kopaonik Block and the Ridge Unit, *VZWB* Vardar Zone Western Belt, *JB* Jadar Block, *DIE* Drina–Ivanjica Element, *DOB* Dinaridic Ophiolite Belt, *EBDMU* East Bosnian–Durmitor Megaunit. **c** Geology of the wider surrounding of the town of Sjenica (part of the simplified map by Živaljević et al. 1983). Legend: 1 Alluvial, 2 Neogene sediments, 3 Ophiolitic mélange (3a peridotite and basite), 4 Middle to Upper Jurassic radiolarites with intercalated turbidites and mass transport deposits, 5 Lower Jurassic red limestone, 6 in general Upper Triassic massive and bedded limestones, 7 Middle Triassic limestone, 8a normal fault, 8b supposed fault, 8c erosional boundary, 9 localities: **a** Krš Gradac **b** Strmenica **c** Brajska reka, 10 Trijebinska Reka section (*asterisk*)

(Gawlick et al. 2016, 2017) is an important segment within the Alpine–Dinarides–Albanides–Hellenides Orogenic System (e.g., Jones and Robertson 1991; Bortolotti et al. 2006; Gawlick et al. 2008; Kiliyas et al. 2010; Ozsvárt et al. 2012; Kiliyas et al. 2016). The most conspicuous feature of this belt is a Middle–Upper Jurassic ophiolitic mélange with large gravity slides/blocks of varying origin and huge bodies of ultramafic masses (Dimitrijević et al. 2003; Karamata 2006; Haas et al. 2011; Kovács et al. 2011; Gawlick et al. 2016, 2017).

Investigations of the rock assemblage, which was first referred to as the “Diabas–Hornstein Formation” or “Diabashornsteinschichten” (e.g., Ampferer and Hammer 1918; Hammer 1923), began in Serbia before the 1920s, the focus of studies being its age-determination (Triassic or Jurassic). It was considered a normal volcanic-sedimentary formation and this opinion persisted for a long time (see in Dimitrijević et al. 2003). Intensive studies were performed during the time of geological mapping for the Basic Geological Map of the SFRY (scale 1:100,000) between 1960 and 1990, when these deposits were called the “Diabase–Chert Formation” (e.g., Živaljević et al. 1983).

Dimitrijević and Dimitrijević (1973, 1979) summarized the general characteristics of this rock assemblage in the Inner Dinarides, calling it ophiolitic mélange for the first time in the area of SW Serbia, and suggesting its sedimentary origin. Karamata et al. (1999) interpreted an oceanic trench complex as the depositional environment; in contrast with other authors (e.g., Schmid et al. 2008), they supposed a more or less para-autochthonous position of the mélange. Later, Dimitrijević et al. (2003) described a chaotic association of shallow-marine to deep-sea sedimentary rocks and mafic to ultramafic rocks as an olistostrome/mélange and interpreted this block-in-matrix texture as slope sediments. In the above-mentioned papers of Serbian authors, all the ophiolitic rocks were interpreted as large blocks and/or olistoplaeae within the mélange. Gawlick et al. (2016, 2017)

distinguished two types of succession within the area of the DOB: (1) the underlying Triassic to Upper Jurassic para-autochthonous sedimentary sequences formed by imbrication and nappe overthrusting within the continental margin, and (2) the overlying Middle Jurassic mélanges (sedimentary mélange mainly with Triassic and Jurassic clastic components) deposited in the foreland basins of the advancing nappe stack formed due to the westward-prograding ophiolite obduction.

Intensive and comprehensive geological investigations and detailed mélange analyses were initiated in the DOB after the first papers of Gawlick et al. (2007, 2009). These studies revealed the complexity caused by the multiple resedimentation processes and multiphase deformation, leading to different and commonly contradictory interpretations for the genesis of the studied rock assemblages (discussed by Gawlick et al. 2017).

After reconnaissance studies in the vicinity of the town of Sjenica located in the south-easternmost parts of Zlata Mt. (Gawlick et al. 2009), we carried out detailed field investigations and sampling along a section on the eastern side of the Trijebinska Reka valley (Fig. 1c). The section exposes part of the para-autochthonous basement of the ophiolite mélange. Our investigations permitted the chronostratigraphic assignment and provided data on the litho- and bio-facies characteristics, as well as the sedimentological features of the succession recording a significant part of the history of the Neotethys margin evolution. Since only a few similar exposures are known in the Inner Dinarides, and the number of the detailed, comprehensive studies is very limited, the results are particularly important for the reconstruction of the evolution of the Adriatic margin of the north-western Neotethys Ocean as a whole.

Geological setting and earlier investigations in the Sjenica area

In the central parts of the DOB, especially in the area of Zlata Mt., the widely exposed ophiolite mélange contains clasts of variable lithology (pelagic carbonates, radiolarites, ophiolitic rocks, albite granites, etc.) and variable size (from millimeter to hundreds of meter) in a shale, radiolaritic marl, and radiolarite matrix. In the neighborhood of the town of Sjenica, this rock assemblage was named the “Sjenica mélange” (Gawlick et al. 2009). More or less silicified, bedded limestones also occur in the same area, either as redeposited blocks in the mélange or as parts of para-autochthonous sedimentary successions (Gawlick et al. 2017).

During the mapping project of Thematic Geological Maps of Serbia (1:50,000), which began in the late 1980s and was based on lithostratigraphic principles, Dimitrijević and Dimitrijević (1991) introduced the name Grivska Formation

for grey, thin-to-medium cherty bedded limestones with thin marl and clayey limestone interlayers. According to their interpretation, it represents a hemipelagic facies and they assigned it to the Ladinian. Later, based only on macroscopic attributes, regardless of their generally unknown age and without any detailed microfacies investigations, the term “Grivska Formation” was used in a confusing and misleading way until the recent work of Gawlick et al. (2017) and Sudar and Gawlick (2018) for all Middle Triassic (Ladinian) to Middle (?Upper) Jurassic grey cherty limestone successions in the DOB (e.g., Dimitrijević 1997; Radovanović et al. 2004; Chiari et al. 2011), and also in the Vardar Zone Western Belt (Toljić et al. 2013).

After reinvestigation of the Grivska Formation in its type locality and in adjacent areas of the DOB, a new amended definition was presented by Gawlick et al. (2017) and Sudar and Gawlick (2018). According to the new definition, the Grivska Formation is characterized by radiolarian- and filament-bearing wackestones, without any platform-derived components, Late Triassic (early Carnian to Rhaetian) in age; it is known only as blocks in the ophiolitic mélange. For the other Triassic grey cherty limestones occurring in the DOB and for the Kopaonik area in the Vardar Zone (in the sense of Karamata 2006; Gawlick et al. 2017), new formations were introduced by Schefer et al. (2010), Missoni et al. (2012), Sudar et al. (2013) and Gawlick et al. (2017).

Two new radiolarite units were defined from the Middle and Upper Jurassic para-autochthonous sequences of the DOB (Gawlick et al. 2017). Grey cherty limestones of Jurassic age also occur but they have not yet been differentiated, defined, and reviewed in a lithostratigraphic sense.

In the initial studies of the “Diabase–Chert Formation” (up to the 1980s) in the Sjenica area, the succession of the Trijebinska Reka section (black asterisk in Fig. 1c) was the object of very contradictory opinions. Jovanović et al. (1979) considered it as a limestone-chert series, with rare intercalations of diabase, tuffaceous sediment, siltstone and marl, undoubtedly indicating its volcanic-sedimentary genesis, and did not assign it to the “Ophiolitic mélange”. Working on the Geological Map of Serbia (1:50,000), Radovanović et al. (1996) suggested that the exposed bedded limestone sequence should be treated as a separate unit (without suggesting any name) within the complex of the “Diabas–Chert Formation” (i.e., in the Ophiolite Mélange). Radovanović et al. (2004) on the sheet Prijepolje 2 (Geological Map of Serbia, scale 1:50,000), including the area of our study, distinguished the “Ophiolite Mélange” and the “Grivska Formation” as separate units.

Several sections similar to that in the Trijebinska Reka valley occur in the vicinity of the town of Sjenica. One of them is Brajska Reka near the village of Aljinovići (locality c in Fig. 1c) and another is Strmenica on Jadovnik Mt. (locality b in Fig. 1c). In the first section, Jurassic bedded

limestones with resedimented bioclasts and lithoclasts of various ages were classified into an individual lithostratigraphic unit (without any specified name), as a member of the “Diabase–Chert Formation” (Jovanović et al. 1994). Preliminary field investigations of the Lower to Upper Jurassic cherty limestone successions were performed by our Serbian–Hungarian team in the year 2008 in the Strmenica locality, Jadovnik Mt. (locality b in Fig. 1c).

West of Sjenica, in the Krš Gradac section (locality a in Fig. 1c), there is exposed a succession occurring below the ophiolitic mélange. It is made up of Upper Triassic platform carbonates, Lower Jurassic shallow-marine to hemipelagic limestones, and Middle to Upper Jurassic radiolarites with turbiditic interbeds (Radoičić et al. 2009; Vishnevskaya et al. 2009; Gawlick et al. 2009, 2017). This succession was previously interpreted as a tectonic window or a tectonically incorporated sliver/slice (Gawlick et al. 2009). However, according to the latest interpretation of Gawlick et al. (2017), the exposed Upper Triassic to Upper Jurassic sequence belongs to the para-autochthonous succession that is overthrust by the ophiolitic mélange around the Jurassic/Cretaceous boundary.

In the later Serbian literature, the Jurassic cherty carbonate successions in the wider surroundings of Sjenica (localities in Fig. 1c) were wrongly assigned to the “Grivska Formation” (e.g., Dimitrijević 1997; Radovanović et al. 2004). The successions exposed in the above-mentioned localities differ significantly in age and litho- and micro-facies characteristics from those of the amended Grivska Formation (in the sense of Gawlick et al. 2017; Sudar and Gawlick 2018). The Upper Triassic–Middle Jurassic or Lower to Upper Jurassic deposits from these localities should be assigned to one or more new formations not yet defined, which like the Upper Triassic Grivska Formation belong(s) to the para-autochthonous basement of the DOB, i.e., occur(s) below the Middle to lower Upper Jurassic ophiolitic mélange and the ophiolite nappes (Gawlick et al. 2017).

Materials and methods

The studied section, traditionally named the Trijebinska Reka section, is situated on the eastern side of the river valley near the installations of the Sjenica water supply system (N 43°14'5.5" E 19°59'31.4"; Figs. 1, 2).

Sampling for microfacies and micropaleontological studies was carried out in two stages. The measured section with the indication of the sampling points is displayed in Fig. 3. In the course of the first sampling, 87 samples were collected; they are marked by the letter S. This was followed by a second sampling to complement the previous sample series, when 29 samples were collected; they are marked by the letter T. From the red radiolarite in the uppermost part of



Fig. 2 The eastern side of the Trijebinska Reka valley showing the steeply dipping beds in the middle part (Unit 6) of the studied succession

the studied section, three additional samples (BR3, VL-14, GBR1) were selected. In total, 102 thin-sections 24×46 mm in size and 60 thin-sections 50×50 mm in size, were analyzed. Based on the thin-sections, ten samples, which were the richest in calcareous microfossils, were treated with glacial acetic acid. Six samples (T7, T10, T29, BR3, VL-14 and GBR1) were dissolved in approx. 3–5% HF (nine parts distilled water and one part concentrated HF (48%)), following the standard laboratory procedures of Pessagno and Newport (1972). Thereafter, the samples were treated repeatedly in approx. 1–2% HF; thus samples T29 and BR3 yielded some poorly preserved but determinable radiolarian species.

The preparation and microscopic study of the samples were carried out in the laboratories of the Department of Petrology and Geochemistry and the Department of Paleontology of the Eötvös Loránd University (the MTA-ELTE Geological, Geophysical and Space Science Research Group), where all micropaleontological and sedimentological materials and the thin-sections are stored. The imaged radiolarians and sponge spicules presented herein were taken

using a Hitachi S-2600 N type scanning electron microscope at the Hungarian Natural History Museum, Budapest.

Results

General description and subdivision of the studied section

Strongly weathered basalt with several better-preserved pillows in chertified matrix (ophiolitic *mélange*) occurs at the north-eastern end of the studied section (Fig. 3a) exposed on the eastern side of the Trijebinska Reka valley. From chertified shale matrix, radiolarians of Late Bathonian–Early Callovian (UAZ 7) age were found (Djerić 2002). At present, due to a few meters-thick covered interval, the contact between the *mélange* and the studied succession is not visible.

Along the valley an approximately 230-m-thick, continuous, steeply dipping monoclinical succession is exposed

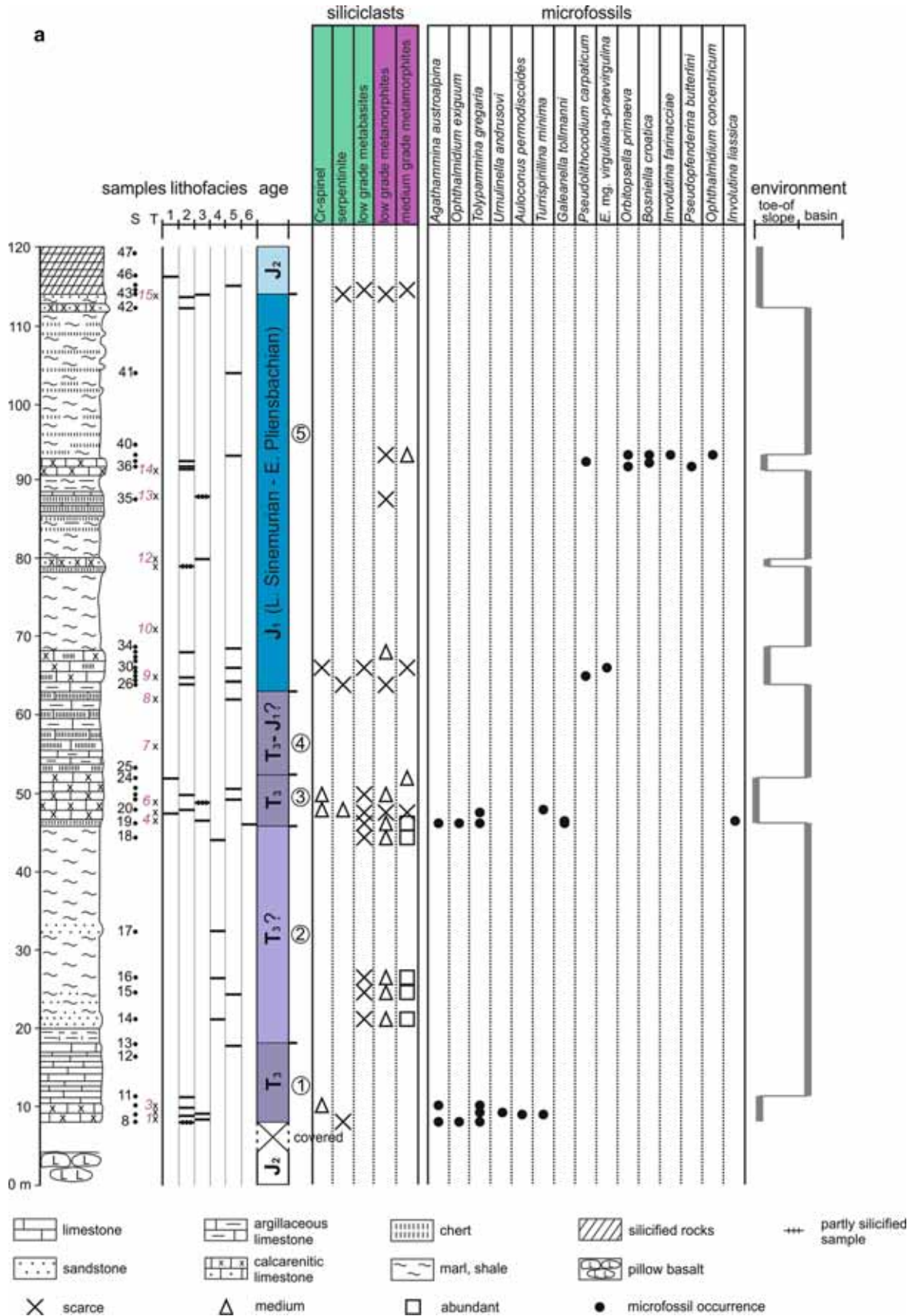


Fig. 3 Lithological column of the studied section with indication of the position of the samples, lithofacies types, chronostratigraphic assignments, and the distribution of the most important age-diagnostic microfossils, the most characteristic siliciclastic components and the interpretation of the depositional environments. The circled numbers 1–8 refer to the distinguished units. *S* samples taken during the first sampling campaign, *T* samples taken during the second sampling campaign, *T*₃ Upper Triassic, *J*₁ Lower Jurassic, *J*₂ Middle Jurassic. **a** lower part of the section. **b** upper part of the section

(Figs. 2, 3). It starts with a thick limestone bed progressing upward into thin-bedded grey limestone. It is followed by an approximately 30-m-thick darker grey, fine-grained siliciclastic sandstone, siltstone, and shale interval. The higher part of the succession (above 125 m) is made up by an alternation of thick-bedded, fining-upward calcarenitic limestone and thin-bedded or platy limestone, argillaceous limestone, or marl. The latter rock types are commonly silicified; they contain thin layers and lenses of chert and are partially locally dolomitized. Red siliceous shale and chert were found in the uppermost part of the studied section (Fig. 3a, b).

Lithofacies types

Based on the field observations and the microfacies investigations, the following lithofacies types (Lf) were distinguished (Fig. 4):

Lf 1 Medium- to coarse-grained packstone to wackestone (“micro-olistostromes”). Along with bioclasts, ooids, cortoids, and peloids, 1–3-mm-sized carbonate lithoclasts usually occur. A small amount of coarser sand-sized and rarely fine gravel-sized siliciclasts were also found at several horizons.

Lf 2 Medium-grained grainstone to packstone. In addition to bioclasts, larger peloids (0.2–0.8 mm) ooids, cortoids, oncoids, and microbial micritic nodules are the typical carbonate grains. A small amount of sand-sized siliciclastic components commonly occurs, mostly in the basal part of the graded beds.

Lf 3 Fine-grained grainstone to packstone. Bioclasts, small peloids (0.05–0.3 mm), cortoids, ooids and intraclasts are the typical carbonate grains. A small amount of fine sand- to silt-sized siliciclasts is commonly present.

In all of the redeposited carbonate rocks described above, fragments of echinoderms (crinoids and echinoids) are usually common. Fragments of bivalves and ostracod shells are also present in several samples. Fragments of calcimicrobes (*Girvanella*-type and *Cayeuxia*-type, microproblematica (*Baccinella* sp., *Pseudolithocodium* and *Thaumatoporella* sp.) and Solenoporacean red algae commonly occur. From among the dasycladalean green algae, *Acicularia* sp., *Anisoporella* sp., *Epimastopora* sp., *Selliporella?* sp. and *Clypeina* sp. were found in small quantities. The

dasycladaleans are fragmented, generally strongly eroded, rounded, and in some cases they appear as the core of cortoids or within larger lithoclasts. Foraminifers commonly occur but usually in a very small number. The specimens are mostly fragmented and/or corroded. In some cases, the foraminiferal specimens occur as individual grains between other grains, but in others they appear in smaller or larger lithoclasts. Locally, the foraminiferal specimens are preserved as the nucleus of ooids, or with cyanobacterial encrustation around them.

The carbonate grains of the above-described redeposited limestone beds were derived from an active carbonate platform; the redeposition took place mostly prior to consolidation of the sediments. In the case of Lf 1, debris flows and grain flows may have been the transporting mechanisms and the toe of a platform foreslope the site of deposition. Lf 2 can be assigned to medium-grained turbidites and may have been deposited in the distal part of the toe-of-slope belt. Lf 3 is a fine-grained turbidite, which may have been deposited in distal toe-of-slope and basinal environments.

Lf 4 Siliciclastic–carbonate rocks; sandstone, siltstone, claystone, marl. The sandstone beds consist of 0.05–0.2 mm-sized siliciclasts predominantly derived from metamorphic rocks, although components derived from acidic magmatic rocks are also present. Radiolarians occur in the claystone/marl beds, which are commonly silicified. This lithofacies type may have been deposited in a hemipelagic basin during periods of intensive terrigenous input.

Lf 5 Carbonate mudstone. There are only a small number of radiolarians, sponge spicules, and very small echinoderm fragments in a micritic matrix; this is hemipelagic to eupelagic basin facies.

Lf 6 Radiolarite, spongiolite. It consists predominantly of radiolarians and/or sponge spicules and is a eupelagic basin facies.

The lithofacies categorization of every studied sample, the occurrences of the age-diagnostic fossils and the siliciclastic components, and the interpretation of the depositional environment are displayed in Fig. 3a, b.

Based on the origin of the grains, two main groups of siliciclast are distinguished (Fig. 3a, b). The first group includes minerals and rock-types of a magmatic–anchemetamorphic part of a normal ophiolitic rock series (serpentinite and microcrystalline chlorite derived from glass alteration), Cr-spinel and strongly altered, chloritized mafic magmatic rocks (variolitic and porphyric basalts, dolerite). Some of the sedimentary–metasedimentary rock types may also belong to an ophiolitic sequence (siltstone, metasiltstone, radiolarite, metaclaystone). The other group of siliciclasts was derived from low- to medium-grade metamorphic rocks: chlorite schist, phyllite, quartzite, chloritic metasandstone, mica schist, muscovite schist, chlorite-bearing mica schist, chlorite phyllite, chloritized biotite, chloritic quartzite,

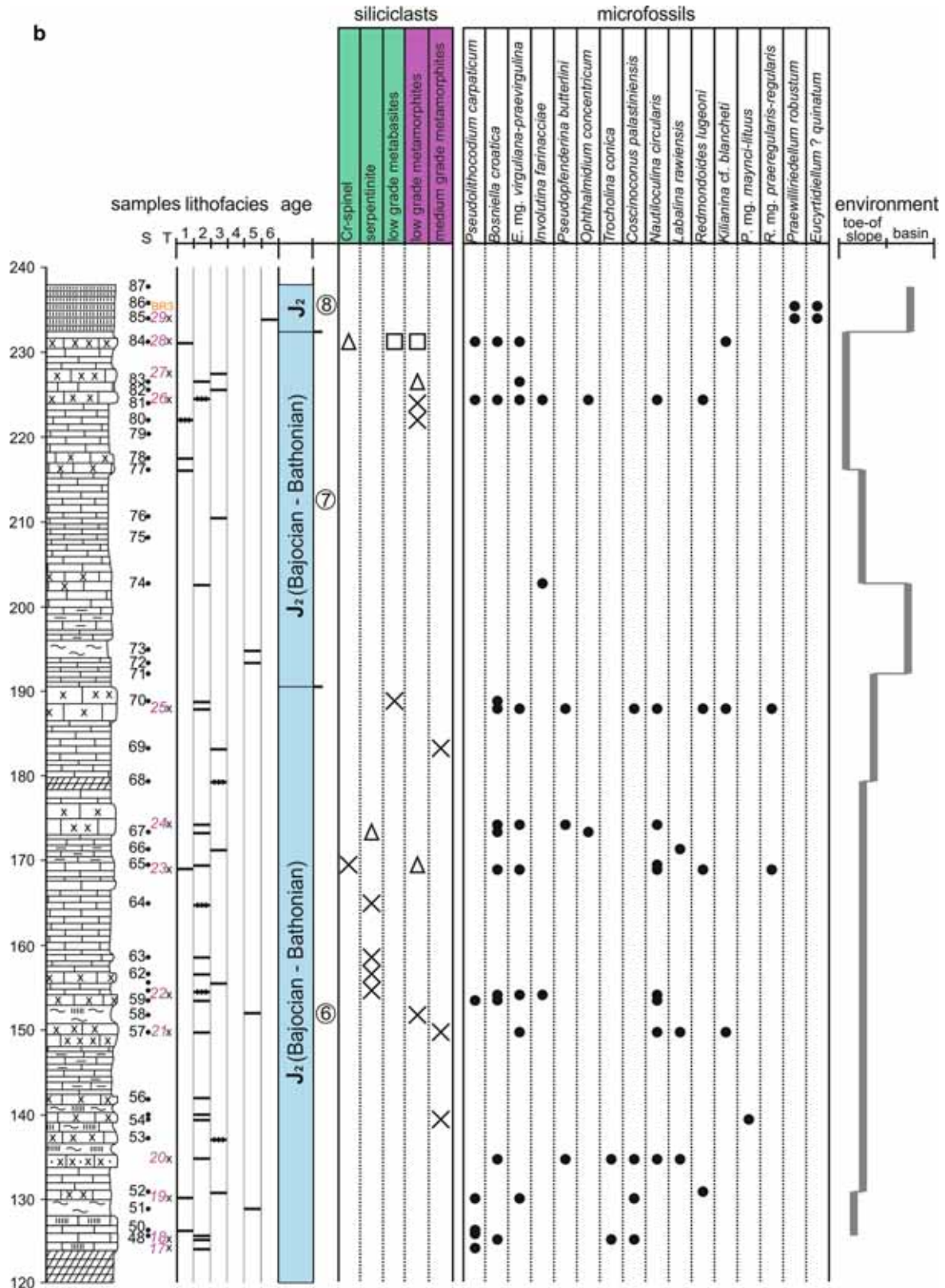


Fig. 3 (continued)

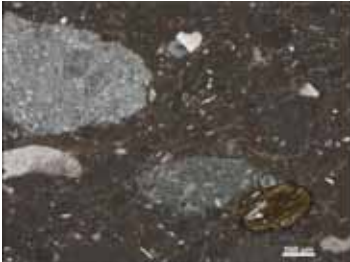
	Lf1 medium to coarse-grained packstone or wackestone	ooids, cortoids, oncoids, peloids, bioclasts, clasts of various lithology	fragments of echinoderms, calcareous sponges, foraminifera, calcimicrobes (<i>Ortonella</i>)	minor debris flow or grain flow; toe-of slope deposit
	Lf2 medium-grained grainstone or packstone	peloids, ooids, intraclasts, bioclasts, cortoids, oncoids, microbial nodules	fragments of echinoderms, foraminifera, dasycladalean algae, calcimicrobe (<i>Girvanella</i> , <i>Cayeuxia</i>)	medium-grained turbidite; toe-of-slope deposit
	Lf3 fine-grained grainstone or packstone	small peloids, cortoids, ooids, intraclasts	fragments of echinoderms, molluscs, foraminifera, ostracods	fine-grained turbidite or the middle portion of a medium-grained turbidite; toe-of-slope to basin
	Lf4 siliciclastic-carbonate rocks sandstone, siltstone, claystone, marl	quartz and carbonate grains (50–200 μm) angular to subrounded lithoclasts /in some horizons/	radiolarians /in some shale beds/	toe-of-slope and hemipelagic to pelagic basin
	Lf5 carbonate mudstone	scattered bioclasts	radiolarians, sponge spicules, small fragments of echinoderms	pelagic basin
	Lf6 radiolarite, spongiolite	large amount of bioclasts	radiolarians, sponge spicules	pelagic basin

Fig. 4 Characteristic features of the lithofacies types and their supposed depositional environment

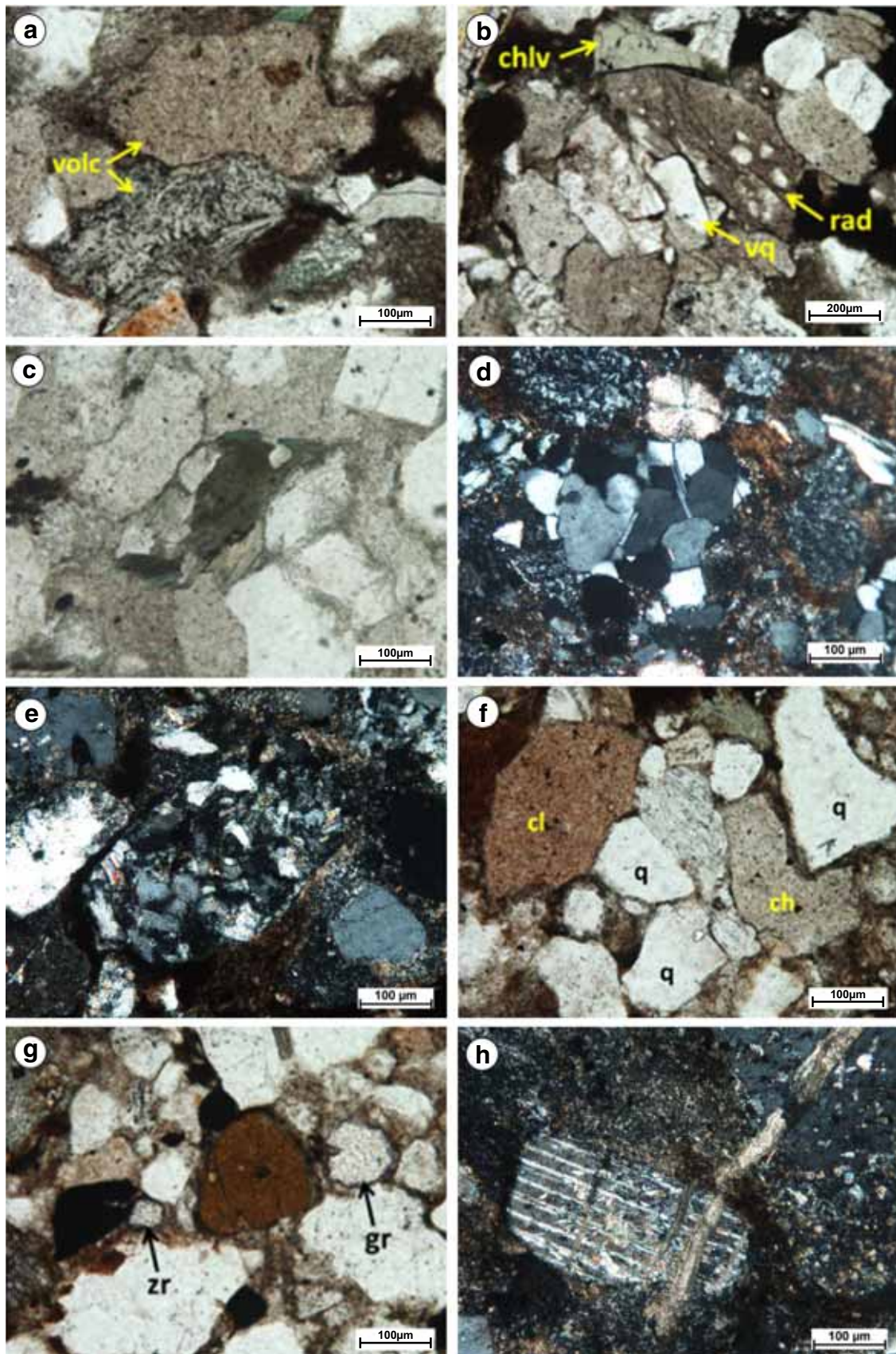


Fig. 5 Typical components of the lower siliciclastic interval. **a** Fine-grained volcanic and volcanoclastic (volc) grains with thin feldspar laths in polymictic sandstone (sample S15; PPL). **b** Radiolarian claystone (rad), claystone, siltstone, acid volcanite with resorbed quartz (vq) in fine-grained groundmass and green chloritized volcanic glass (chlV) clasts in polymictic sandstone (sample S15; PPL). **c** Biotite chlorite schist grain (green in the middle) in polymictic sandstone (sample S15; PPL). **d** Chloritic (thin elongated bluish grains) quartzite (in the middle), with isometric quartz grains (grey) in polymictic sandstone (sample DRF1-15; XPL). **e** Chlorite (green)-rich metasandstone grain (in the middle) in polymictic sandstone (sample S15; PPL). **f** Wavy muscovite flakes (in the middle), angular quartz (q), claystone (cl), and chert (ch) grains in polymictic sandstone (sample S15; PPL). **g** Heavy mineral enrichment (placer) in polymictic sandstone. Tourmaline (dark brown in the middle), garnet (gr), zircon (zr) and opaque mineral (black) (sample S15; PPL). **h** Sericitized plagioclase grain (twinned) crossed by carbonate vein in polymictic sandstone (sample S15; XPL)

gneiss, and biotite. Only a few of these rock fragments (e.g., metasandstone) contain relics of the pre-metamorphic magmatic or sedimentary rocks. Other components such as acidic non-zoned (intrusive) plagioclase, sericitic orthoclase, zircon, tourmaline, and some microcrystalline quartz were probably derived from acidic magmatic rocks (granitoids and rhyolites).

Litho- and bio-facies characteristics and chronostratigraphic assignment

As to its lithofacies characteristics, the whole succession below the red shale and radiolarite unit is rather uniform; it is made up of an alternation of toe-of-slope and basinal facies although, based on biostratigraphic data, it represents a long time-range, from the Late Triassic to the Middle Jurassic. Since we could not assign this succession or segments of it to the previously defined lithostratigraphic units (e.g., Gawlick et al. 2017) and we did not want to define new ones on the basis of a single section, we subdivided the studied section into eight informal units, which are based mostly on the microfacies assemblages (Foraminifera, Chlorophyta, Chlorophyta Radiolarians, Porifera, Polychaete, and Inceratae sedis) but also taking into account the lithofacies characteristics.

The chronostratigraphic assignment of the studied section is based on microfossils. For the biostratigraphic evaluation, the foraminifers were mostly used, but the age-diagnostic value of radiolarians and other microfossil groups was also considered. The fossil assemblage of the toe-of-slope facies is evidently mixed; it may contain both autochthonous and allochthonous (redeposited) elements. This aspect should be taken into account for the age evaluation and interpretation of the habitat of the fossils.

For the characterization of these units, we describe first the lithological features and the most typical siliciclastic components (Figs. 5, 6). The microfossils (Figs. 7, 8, 9, 10,

11) are listed in descending order of their frequency. For the systematic position, the selected synonymy, the stratigraphic range, and the ecological needs of the mentioned species, see Online Resource 1.

Unit 1 The lowermost bed-set of the measured section (8–18 m; samples S6–13, T1–3) is made up of a thick, carbonate turbidite bed (Lf 2, Lf 3) that is overlain by a thin-bedded brownish grey limestone (Lf 5). In a bioclastic wackestone bed a small serpentinite grain and in a bioclastic, peloidal grainstone bed, several Cr-spinel grains were found.

The microfossil associations consist mostly of echinoderms and foraminifers. Bivalves and ostracods are relatively common. A few fragments of *Thaumatoporella* sp. (Fig. 7a) are also present. The foraminiferal fauna is moderately rich, but relatively diverse. It is characterized by the dominance of miliolinids as *Agathammina austroalpina*, *Ophthalmidium exiguum*, *Decapoolina schaeferae*, *Miliolipora cuvillieri*, *Paraophthalmidium carpaticum* and *Urnulinella andrusovi* (Fig. 7b–g). The *Planiinvoluta carinata* (Fig. 7h) and *Tubiphytes*-like (*Carniphytes*? sp.) forms (Fig. 8i) are relatively common. The agglutinated foraminifers are represented by some specimens of the genera *Glomospira*, *Endothyra*, *Trochammina*, and *Valvulina*. The *Nodosariidae* are rare; few *Nodosaria*, *Lenticulina*, *Lingulina* and *Polarisella* ex. gr. *elabugae* (= *Frondicularia woodwardi*) occur. Only involutinids *Auloconus permodiscoides* (Fig. 7j) could be recognized.

In the microfossil assemblages, elements of a reef (*Decapoolina*, *Planiinvoluta*, *Urnulinella*, *Thaumatoporella*) and deeper-water community (*nodosariids*, sponges) are mixed indicating resedimentation (Fig. 7; Online Resource 1).

The foraminiferal fauna indicates a Late Triassic age. The *U. andrusovi* and the genus itself has been known only from the Carnian (Senowbari-Daryan 2016), while *D. schaeferae* and *A. permodiscoides* only from the Norian–Rhaetian. The genus *Urnulinella* belongs to the “*Cucurbita* group”, which mostly appears in the Carnian, but some representatives lived in the Norian–Rhaetian interval (e.g., Senowbari-Daryan 2016). According to several authors (e.g., Bernecker 2005; Senowbari-Daryan 2016), the organisms, including the foraminifers of the Carnian and the Norian–Rhaetian reef systems, are significantly different. Accordingly, the most probable age of this interval is latest Carnian–Rhaetian.

Unit 2 This is a siliciclastic interval (18–47 m, samples S14–19). The carbonate layers of Unit 1 are overlain by dark brown shale with a sharp boundary. This is followed by a grey, fine-grained siliciclastic sandstone interval that gradually progresses upward into siltstone and shale (Lf 4).

In the lower part of this interval, in a medium sand-sized sandstone bed (sample S15), there occur rock fragments (quartzite, chert, chloritic mica schist, muscovitic mica schist, chloritized intersertal basalt) and mineral fragments

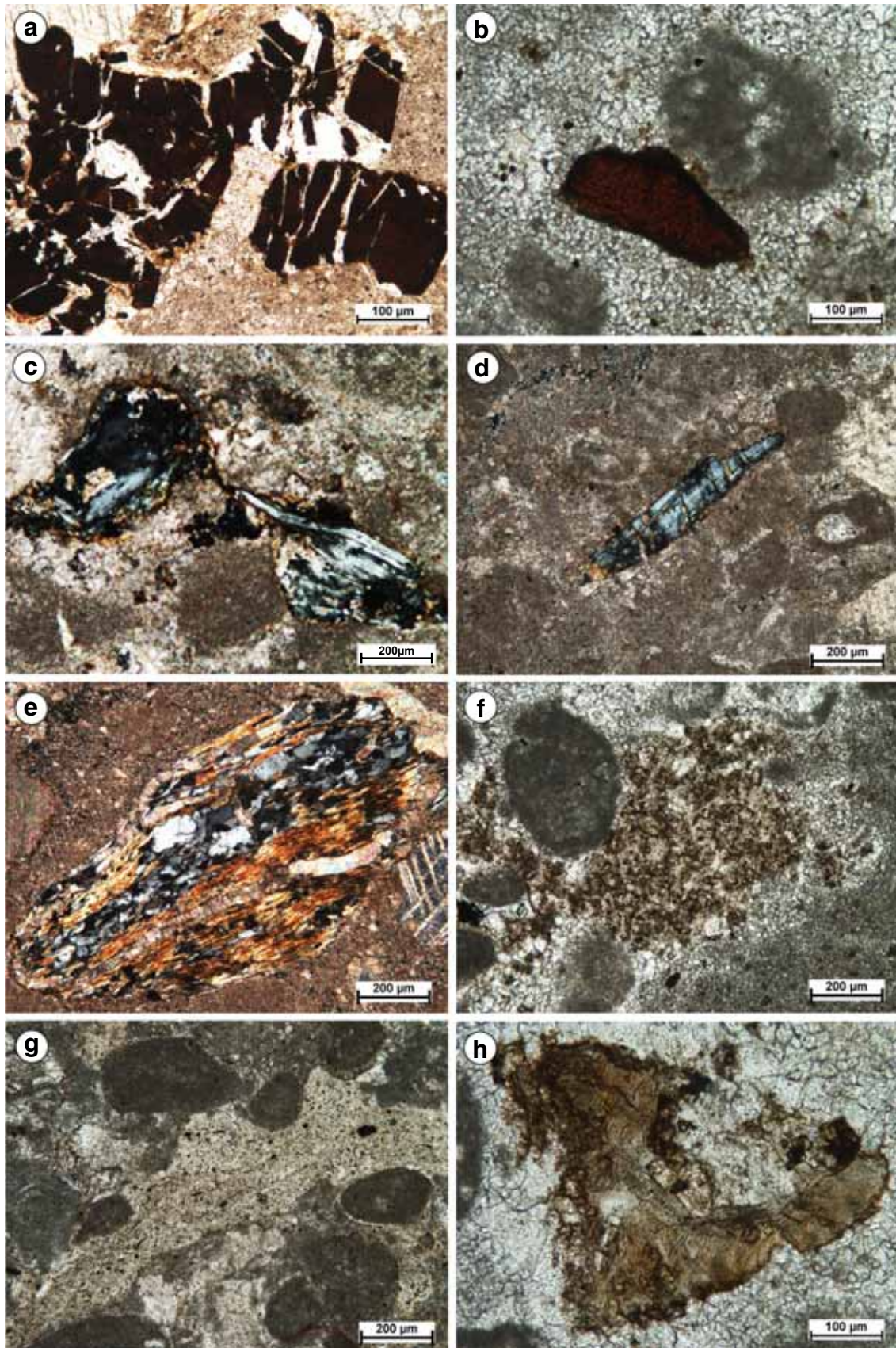


Fig. 6 Typical siliciclastic components of redeposited limestone beds. **a** Large crackled Cr-spinel aggregate (reddish-black) in limestone (sample T28; PPL). **b** Angular Cr-spinel crystal grain (dark red) in limestone (sample S30; PPL). **c** Strained wavy serpentinite-chloritite fragment (grey) in limestone (S20; XPL). **d** Elongated section of a serpentinite-chloritite fragment (grey) in limestone (sample S19; XPL). **e** Well-rounded grain of fine-grained mica schist consisting of wavy micas (colorful) and quartz (grey) (sample T28; XPL). **f** Strongly altered, partly frayed, most probably mafic volcanite (basalt, brown in the middle) in limestone (sample S30; PPL). **g** Siltstone fragment (lighter fine-grained ribbon) suffered plastic deformation in limestone (sample S19; PPL). **h** Strongly contorted biotite aggregate (greenish) in limestone (sample S30; PPL)

(acidic plagioclase, orthoclase, biotite, and muscovite), including heavy mineral grains (tourmaline, garnet, zircon) (Fig. 5). In a fine-grained sandstone bed (S17), along with chert fragments, metamorphic quartz and quartzite, a few plagioclase, orthoclase and microcline grains, together with metasiltstone and metaclaystone lithoclasts, were encountered.

Radiolarians (Fig. 8k) and sponge spicules are common in this unit. Other microfossils are very scarce; a few echinoderm fragments and recrystallized (silicified and dolomitized) foraminifers (? *Lingulina* sp. (Fig. 8l), *Lenticulina* sp.? *Glomospira* sp.) could be recognized. No age-diagnostic microfossils were found.

Unit 3 In a 5-m-thick interval (47–52 m, samples S19–24, T4–6) the redeposited toe-of-slope facies (Lf 1–3) and the basal facies (Lf 5–6) alternate.

In the basal part of this bed-set, in bioclastic, carbonate lithoclastic wackestone, a few sand-sized fragments of metamorphic quartzite, chloritic quartzite, mica schist, and acidic volcanite (magmatic quartz in microcrystalline quartz matrix) were observed (sample T5). A few small serpentinite and larger Cr-spinel grains, fragments of mica schist, and chloritite were found in the overlying layers.

In the toe-of-slope facies (Lf 1–3), besides fragments of echinoderms, sponge spicules and radiolarians, relatively diverse foraminiferal faunas, and algal associations occur. In the basin facies (Lf 5–6), the microfossil content is very similar to that of the previous interval.

Agglutinated foraminifers as *Valvulina* spp. (e.g., *V. azzouzi*), *Textularia* spp. *Trochammina* spp., *Glomospira* spp., *Ammobaculites* sp., *Pfenderina* sp., *Endothyra* sp. and *Duotaxis metula* are dominant (Fig. 8a–g). The sessile foraminifers *Tolypammina gregaria*, *Planiinvoluta carinata*, and *Placopsilina* sp. are also common (Fig. 8h, i). The miliolinids are represented mostly by *Ophthalmidium* spp. (*O. triadicum*, *O. exiguum*, *Galeanella tollmanni*, and *Arenovidalina chialingchiangensis* (Fig. 8j–o). Few broken specimens of *Turrspirillina minima* and *Parvalamella friedli* occurred (Fig. 8p, q). Stromatoporoids and reef-dweller tubular-shaped problematical microfossils as *Thaumatoporella* sp.

and *Actinotubella gusici*, plus sphinctozoan sponge *Salzburgia variabilis* are relatively common (Fig. 8r–u).

The associations of the aforementioned forms indicate a reefal environment. Deeper-water foraminifers as different Nodosariidae (*Austrocolomia* cf. *rhaetica*, *Nodosaria* spp., *Pseudonodosaria* sp., *Nodosinelloides* sp., *Lingulina* sp., *Lenticulina* sp. and *Polarisella* ex. gr. *elabugae*) are also present in small quantity (Fig. 8v–z).

The microfossils indicate a Late Triassic, Norian–Rhaetic age.

Unit 4 The next interval (52–63 m; samples S25, T7–8) consists of cherty limestone. In the usually strongly silicified rocks, only sponge spicules and radiolarians could be recognized in thin-section. However, the acetolysis of one sample (54 m; T7), provided a relatively diverse foraminiferal fauna. The majority of the specimens are preserved as moulds, which allowed only generic classification. The following, mostly nodosariid forms, were identified *Ichthyoholaria*, *Lingulina*, *Lenticulina*, *Nodosaria*, *Glomospira*, *Pravoslavlevia*, and *Trochammina*. These microfossils indicate a deeper-water environment, but they have no age-diagnostic value.

Unit 5 This 50-m-thick interval (63–113 m; S26–43, T9–16) is characterized by the alternation of carbonate turbidites (Lf 2 and 3) and more or less silicified red shale (Lf 5) bed-sets.

In the redeposited carbonate bed in the lowermost part of this unit (63–68 m), a few chloritite-serpentinite fragments (S26), metadolerite, Cr-spinel, and biotite (S30, Fig. 6b, f, h) grains were identified. Another redeposited carbonate bed (90–93 m) contained mm-sized fragments of chlorite schist, chloritic metasandstone, and mica schist (S38). Chlorite schist, mica schist, serpentinite clasts, and biotite were encountered in the basal part (112–113 m; S43, 44, 45) of a carbonate turbidite bed-set in the upper part of this unit (112–113 m; S43, 44, 45).

In the commonly dolomitized and silicified rocks of this interval, radiolarians and sponge spicules could be recognized. However, in some resedimented beds (91–93 m; sample S38 and 112 m; sample S42), a relatively large number of microfossils were found. In these beds, fragments of echinoderms, algae, calcimicrobes, and foraminifers are common; the shells of bivalves and ostracods are very rare. Among the foraminiferal fauna, the agglutinated forms are the most abundant and diverse. The most common forms are the specimens of *Textularia*, *Trochammina*, and *Valvulina*, whereas genera *Ammobaculites*, *Glomospira*, and *Verneuulinella* are less common; the encrusting *Placopsilina* also occurs (Fig. 9a–d). In a small quantity, characteristic Jurassic larger agglutinated forms could be recognized, namely *Everticyclammina* mg. *virguliana*–*praevirguliana*, *Siphovalvulina* gr. *variabilis*, *Orbitopsella primaeva* (Fig. 9f–g), and *Bosniella* (= *Mesoendothyra*) *croatica* (Fig. 10e–h, m). The

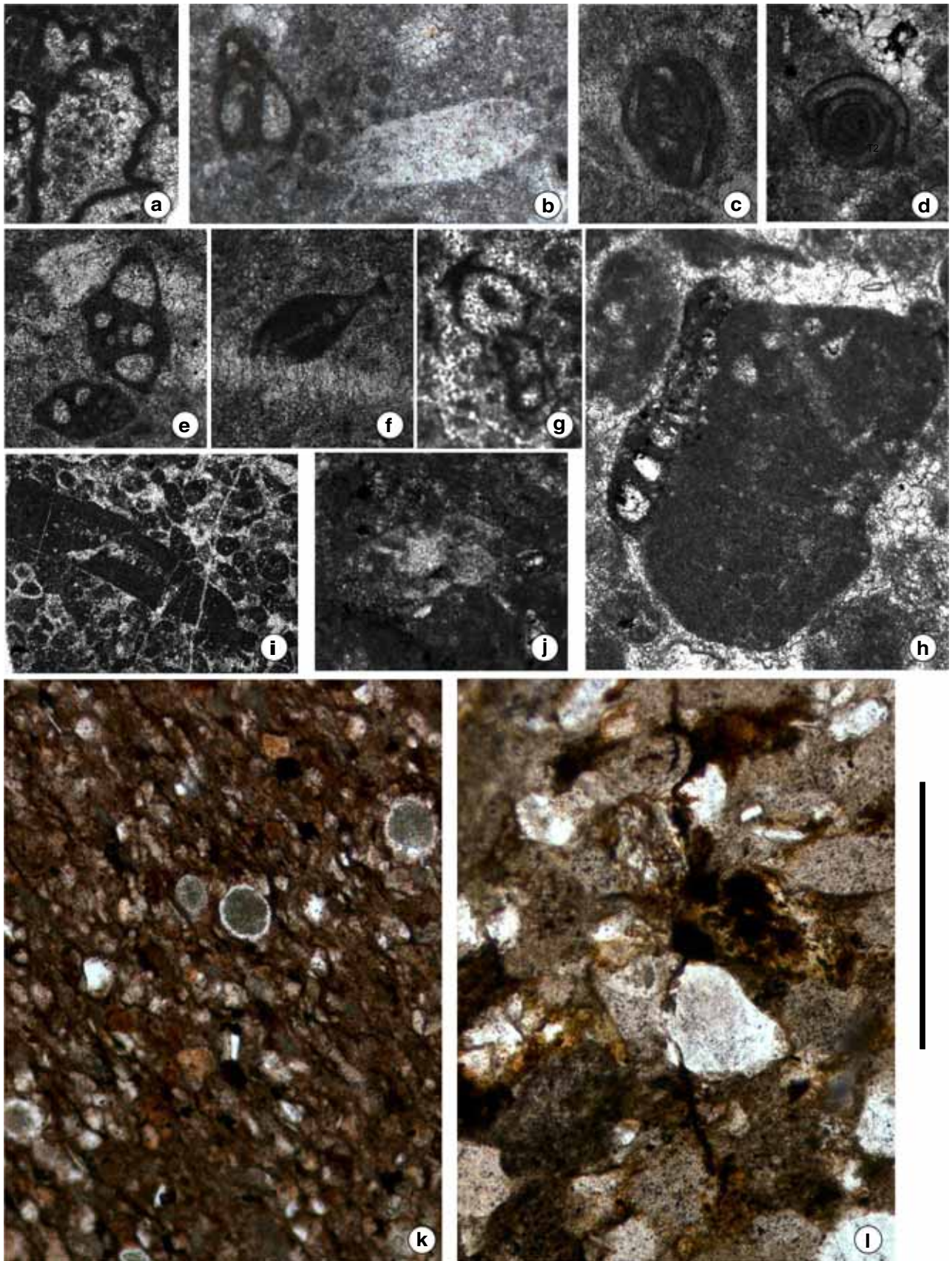


Fig. 7 a–j Characteristic microfossils from the interval 8–12 m (samples S6–12, T1–3) and figures k, l from the interval 12–47 m (samples S13–18). The scale bar is 500 µm, except for figures a and i, where it is 1250 µm. **a** *Thaumatoporella* sp., sample S8b. **b**, **c** *Agathammina austroalpina*, sample S8b. **d** *Ophthalmidium exiguum*, sample S8b. **e** *Decapopolina schaeferae* (below) and *Miliolipora cuvillieri*, sample S8b. **f** *Paraophthalmidium carpaticum*, sample S8b. **g** *Urnulinella andrusovi*, sample T2. **h** *Planiinvoluta carinata*, sample S8. **i** Tubiphytes-like (*Carniphytes?* sp.) form, sample T2. **j** *Aulococcus permodiscoides*, sample S9. **k** Wackestone with radiolarians and sponge spicules, sample S16. **l** siliciclastic carbonate sandstone with recrystallized (silicified) foraminifers (*Lingulina* sp.), sample S18

nodosariids (*Protonodosaria*, *Nodosaria*, *Dentalina*, *Lenticulina*, *Marginulina* occur in a low number but regularly (Fig. 9i, j). The miliolinids are represented only by corroded *Agerella martana* (Fig. 9k), *Labalina* sp. and the encrusting *Planiinvoluta carinata*. The Middle Liassic *Involutina farinacciae* (Fig. 9l) also occurs. Rivulariacean-like cyanobacteria, *Thaumatoporella parvovesiculifera*, *Steinmanniporella?* sp. and Solenoporacea fragments were found in a few beds (Fig. 9l, n–p). Sections of *Carpathiella triangulata* (Fig. 9q) could be recognized.

Some of the microfossils (larger foraminifers, siphons, algae) are characteristic of inner-platform, back reef–reef environments, whereas others (nodosariids, radiolarians) indicate deeper-water ones. The low number of the microfossils and relatively large clasts of fragile filamentous algae suggest basinal and toe-of-slope environments located relatively close to carbonate platform environments. The co-occurrence of *Everticyclammina* mg. *virguliana*–*praevirguliana*, *Orbitopsella primaeva*, and *Involutina farinacciae* indicate late Sinemurian–early Pliensbachian age (see Online Resource 1).

Unit 6 This interval (113–191 m; S44–70, T17–25) starts with strongly silicified rocks (probably of basin facies); thereafter medium- to coarse-grained packstone to wackestone (Lf 1 and 2) become predominant. Only thin carbonate mudstone intercalations (Lf5) occur.

In a sample taken from a turbiditic bed-set in the lower part of this unit (124–128 m; S50) a 3-mm-large chloritic mica schist clast was observed. Higher up, in an interval (128–190 m), which is characterized by the predominance of the coarser and finer-grained redeposited carbonates, a small amount of mica-schist fragments, small serpentinite (?) clasts, chlorite, and biotite grains were found.

In the redeposited calcarenite beds, fragments of calcimicrobes and echinoderms are very common; gastropods, bivalves and foraminifers are also commonly present. Additionally, very few ostracods, bryozoan, brachiopods, and sponge spicules occur sporadically. Radiolarians could be recognized only at 150 m (sample S58), in a radiolarian mudstone (Lf 5) interbed. Fossils of *Siphonales*, dasycladalean algae, and different microproblematica, as *Rivularia lissaviensis*, *R. piae*, *R. sp.*, *Hedstromieia* sp., *Arabicodium*

bicazensis, *Pseudogirvanella?* sp., *Solenopora?* sp., Dasycladacea spp., *Selliporella?* sp., *Anisoporella* sp., *Petrascula* sp., and *Clypeina* sp. are commonly present in this interval (Fig. 9r–bb). Encrusting microproblematica as *Pseudolithocodium carpathicum*, *Bacinella irregularis*, *Thaumatoporella parvovesiculifera* and *Radiomura cautica* as well as foraminifers, namely *Placopsilina* sp., *Subbdellodina haeusleri* and *Tubiphytes* sp., are also relatively common (Figs. 9cc–ee, 10a–d). The agglutinated foraminifers as *Textularia* spp., *Valvulina* spp., *Glomospira* sp., *Trochammina* spp., *Siphovalvulina* gr. *variabilis*, *Riyadhella* mg. *praeregularis*–*regularis*, *Redmondoides lugeoni*, *Ammobaculites* sp., and *Reophax* sp. are prevailing (Fig. 10e–i). Several larger agglutinated forms as *B. mg. croatica*, cf. *Pseudopfenderina butterlini*, *E. mg. virguliana*–*praevirguliana*, *Kilianina blancheti* and *Pseudocyclammina* mg. *maynci*–*lituus* could also be recognized (Fig. 10j–m, q). In the lower part of this interval (126–135 m, samples T18–20), involutinids such as *Trocholina conica* and *Coscinocoonus palastiniensis* low and high-spined forms are relatively common (Fig. 10n–p). From among the miliolinids, specimens of *Nautiloculina circularis* and *Meandrovoluta asiagoensis* are common throughout this interval (Fig. 10j, r). Other porcelanous forms such as *Ophthalmidium concentricum*, *Labalina rawiensis*, and *L. costata* and *Labalina* sp. also occur (Fig. 10s–u). A nubecularid foraminifer (Fig. 10v) similar to that which was classified by Schlagintweit and Velić (2011) to *Bosniella bassoulleti* from the late Aalenian–lower Bajocian was also found.

In some beds, between 170–175 m (samples S65–66, T24), several foraminiferal specimens displaying tests of differentiated, distinct inner dark microgranular and outer light hyalino-radial layers were observed. These forms could be classified as *Protopenneroplis striata* (Fig. 10w) and *Archaeosepta* sp. (Fig. 10x). Nodosariids are subordinate; a few specimens of the genera *Nodosaria*, *Paralingulina* mg. *tenera*, and *Lenticulina* occur. The species occurring in this unit are known from the Middle Jurassic: *Protopenneroplis striata*, *Redmondoides lugeoni*, and *Rivularia piae* from the Aalenian; *Labalina costata*, *L. rawiensis*, *Coscinocoonus palastiniensis*, *Trocholina conica*, *Nautiloculina circularis*, and *Pseudocyclammina* mg. *maynci*–*lituus* from the Bajocian; *Subbdellodina haeusleri*, *Kilianina blancheti*, and *Arabicodium bicazensis* from the Bathonian. *Ophthalmidium concentricum* and *Meandrovoluta asiagoensis*, from the Lower Jurassic–Aalenian period, were identified, while *Riyadhella* mg. *praeregularis*–*regularis* is not known from the late Pliensbachian–early Bajocian interval (see Online Resource 1). Various sub-environments of a carbonate platform were the habitats of most of the species.

In view of the few records of these species from the lower Middle Jurassic, their younger or older occurrences cannot be excluded. Taking into account the above-mentioned

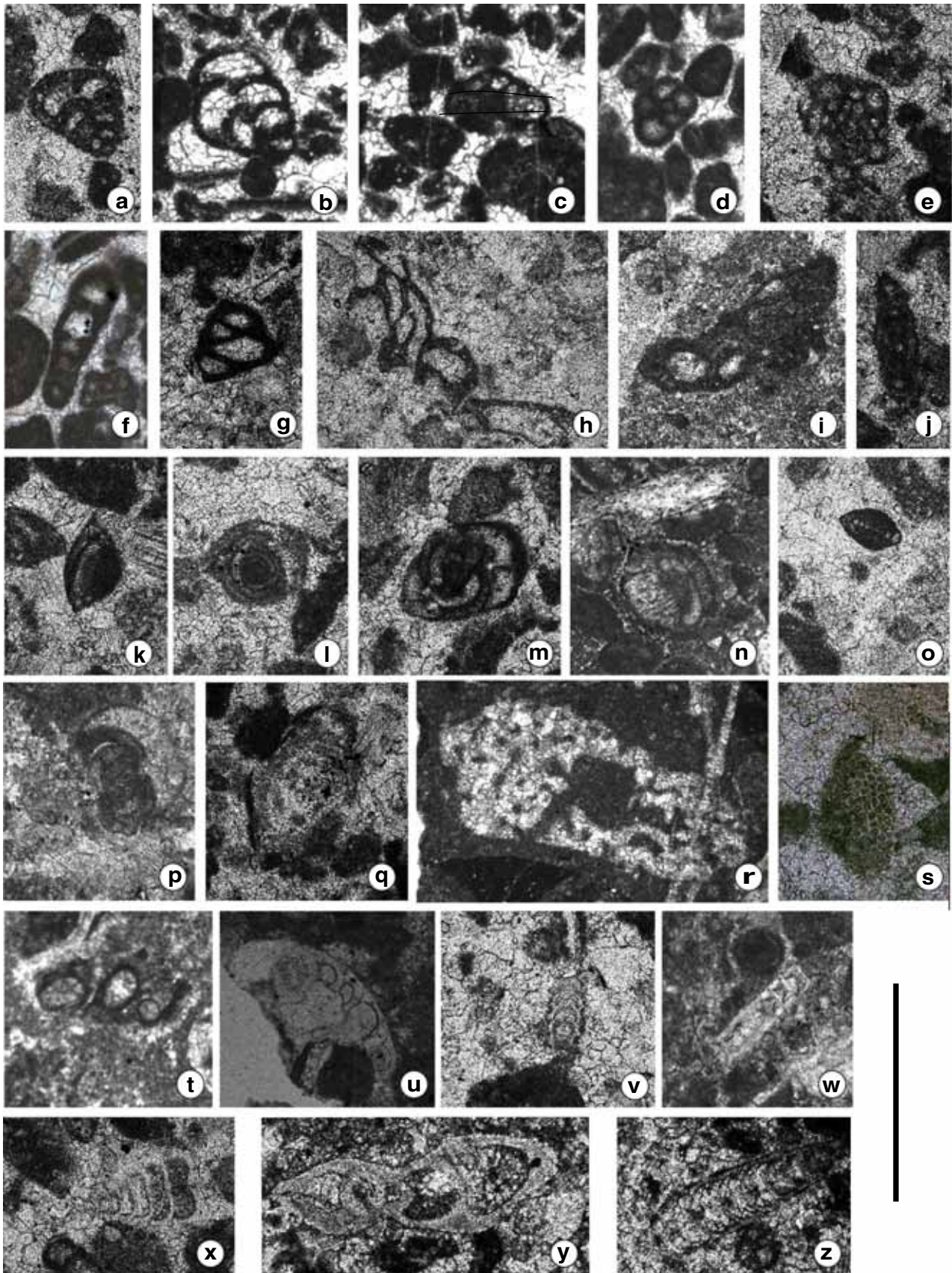


Fig. 8 Characteristic microfossils from the interval 47–52 m (samples S19–24, T4–6). The scale bar is 500 μm , except for **-t**, where it is 1250 μm . **a** *Valvulina azzouzi*, sample T6. **b** *Textularia* sp., sample S23–24. **c**, **d** *Trochammina* sp., sample S23–24. **e** *Glomospira* sp., sample T6. **f** *Ammobaculites* sp. sample S23–24. **g** *Duotaxis metula*, sample T4. **h** *Tolypammina gregaria*, sample T4. **i** *Planiinvoluta carinata*, sample T5. **j**, **k** *Ophthalmidium triadicum*, samples T4 and T6. **l** *Ophthalmidium exiguum*, sample T4. **m**, **n** *Galeanella tollmanni*, samples T4 and T19. **o** *Arenovidalina chialingchiangensis*, sample T4. **p** *Turrispirillina minima*, sample 20. **q** *Parvalamella friedli*, sample T4. **r** stromatoporoid, sample S24. **s** *Thaumatoporella* sp., sample T4. **t** *Actinotubella gusici* sample S24. **u** *Salzburgia variabilis* sample S19. **v** *Austrocolomia* cf. *rhaetica*, sample T4. **w** *Nodosinelloides* sp., sample S20. **x** *Lingulina* sp., sample T4. **y** *Lenticulina* sp., sample T4. **z** *Polarisella* ex. gr. *elabugae*, sample T4

constraints, the age of this interval is taken as Middle Jurassic (?Aalenian–Bajocian–?Bathonian).

Unit 7 This interval (191–233 m) starts with mudstone–wackestone of hemipelagic basin facies (Lf 5) (samples S71–73). It is followed by redeposited siliciclast-bearing fine to coarse calcarenitic bed-sets (Lf 1, 2, and 3) (samples S74–84, T26–28).

In the uppermost part of this unit (216–233 m), mm-sized siliciclasts occur in several redeposited carbonate beds. One of them (S77) contained fragments of muscovitic mica schist, muscovite schist with chloritic quartzite, chlorite phyllite, chlorite-biotite schist, metasiltstone, and metamorphic quartz. The uppermost bed of this interval (samples S84, T28) is made up of coarse sand- to fine pebble-sized (1–5 mm) bioclasts (mostly echinoderm detritus) and lithoclasts (carbonate clasts and siliciclasts). Chromite–Cr-spinel grains, fragments of altered basalt and dolerite, chloritic quartzite, chlorite, and chloritic metasandstone were encountered (T28; Fig. 6a, e).

The redeposited beds are rich in fragments of echinoderms; sponge spicules and radiolarians are also common in some of them. Fragments of gastropods, calcimicrobes, algae, and foraminifers are relatively rare but diverse. From among the microbial remnants and algae, specimens of *Pseudolithocodium carpathicum*, *Bacinella irregularis*, *Th. parvovesiculifera*, *Petrascula* sp., *Solenopora*? and stromatoporoids could be identified (Fig. 11a–e). In the foraminiferal fauna, the agglutinated forms of genera *Ammobaculites*, *Trochammina*, *Valvulina*, *Textularia*, *Glomospira*, and *Reophax*, besides them *Siphovalvulina* gr. *variabilis*, *B. mg. croatica* are dominant (Fig. 11f–i). Few sections of larger foraminifers, namely *Lituosepta recoanensis*, cf. *K. blancheti* and *E. mg. virguliana*–*praevirguliana* also occur (Fig. 11j–m). More nodosariids (*Nodosaria*, *Lenticulina*, *Marginulina*, *Lingulina*) were found here than in the previous interval. The miliolinids are represented by *Nautiloculina circularis*, *Meandrovoluta asiagoensis*, and *Ophthalmidium concentricum* (Fig. 11n–p). The specimens of *Involuntina farinacciae* (Fig. 11q) are relatively common. Few sessile microfossils as *Planiinvolutina carinata*, *Placopsilina* sp.,

and agglutinated polychaetid *Terebella lapilloides* could also be identified (Fig. 11c, r). In various lithoclasts, the Carnian–Rhaetian *Variostoma cochlea* (Fig. 11s) and the Upper Triassic–Lower Jurassic *Involuntina liassica* and *Paralingulina mg. tenera* were recognized (Fig. 11s–u). Based on these observations, it is evident that the co-occurrence of Upper Triassic, Lower, and Middle Jurassic microfossils (see Online Resource 1) can be explained by erosion and redeposition of previously deposited and more to less lithified carbonate components, together with various amounts of siliciclasts, during the Middle Jurassic.

Unit 8 The uppermost part of the measured section (233–239 m) consists of red silicified shale and radiolarite (Lf 6; samples S85–87, T29, BR3), with limestone (peloidal packstone in sample S86) and siliciclastic sandstone (sample S87) interbeds. In the sandstone, along with a large amount of microquartz of volcanic origin, fragments of granite-gneiss, chlorite schist, metasiltstone, and phyllite were recognized.

In the thin-sections of the limestone samples, radiolarians, fragments of echinoderms, and bivalves were found. The only identified foraminifer is the Norian–Rhaetian encrusting *Alpinophragium perforatum* (sample S86; Fig. 11v). The extraction of radiolarians (in sample T29) yielded some sponge spicules (Fig. 12f, g) and isolated foraminifers including *Lenticulina* sp., *Lingulina* sp., *Oberhauserella* sp., and *Duostomina turboidea* (Fig. 11w, x).

The following radiolarian taxa were identified from the samples T29 and BR3: *Praewilliriedellum robustum*, which indicates UA Zones 5–7 (late Bajocian to early Callovian). Both samples contain *Praewilliriedellum convexum*, which is a very common species in entire Middle and Late Jurassic and *Archaeodictyomitra whalenae*, a species that has been known so far from the early Aalenian to early Oxfordian. Beside them, in the sample T29 *Archeodictyomitra prisca* (early Aalenian to early Oxfordian), *Eucyrtidiellum* (?) *quinatum* (early Aalenian to Bathonian) and *Parahsuuum carpathicum* are also present. *Striatojaponocapsa conexas*, *Transhsuum maxwelli*, and *Zhamoidellum* cf. *ventricosum* were extracted from sample BR3. This poorly preserved and low-diversity radiolarian fauna (Fig. 12) suggests late Bajocian to Bathonian age. The Upper Triassic foraminifers found in a limestone interlayer suggest a continuation of redeposition of fine lithoclasts from Triassic limestones.

Discussion

Interpretation of the history and controlling factors of sediment deposition

The studied succession is made up of an alternation of gravity-induced deposits (mostly turbidites) and hemipelagic/

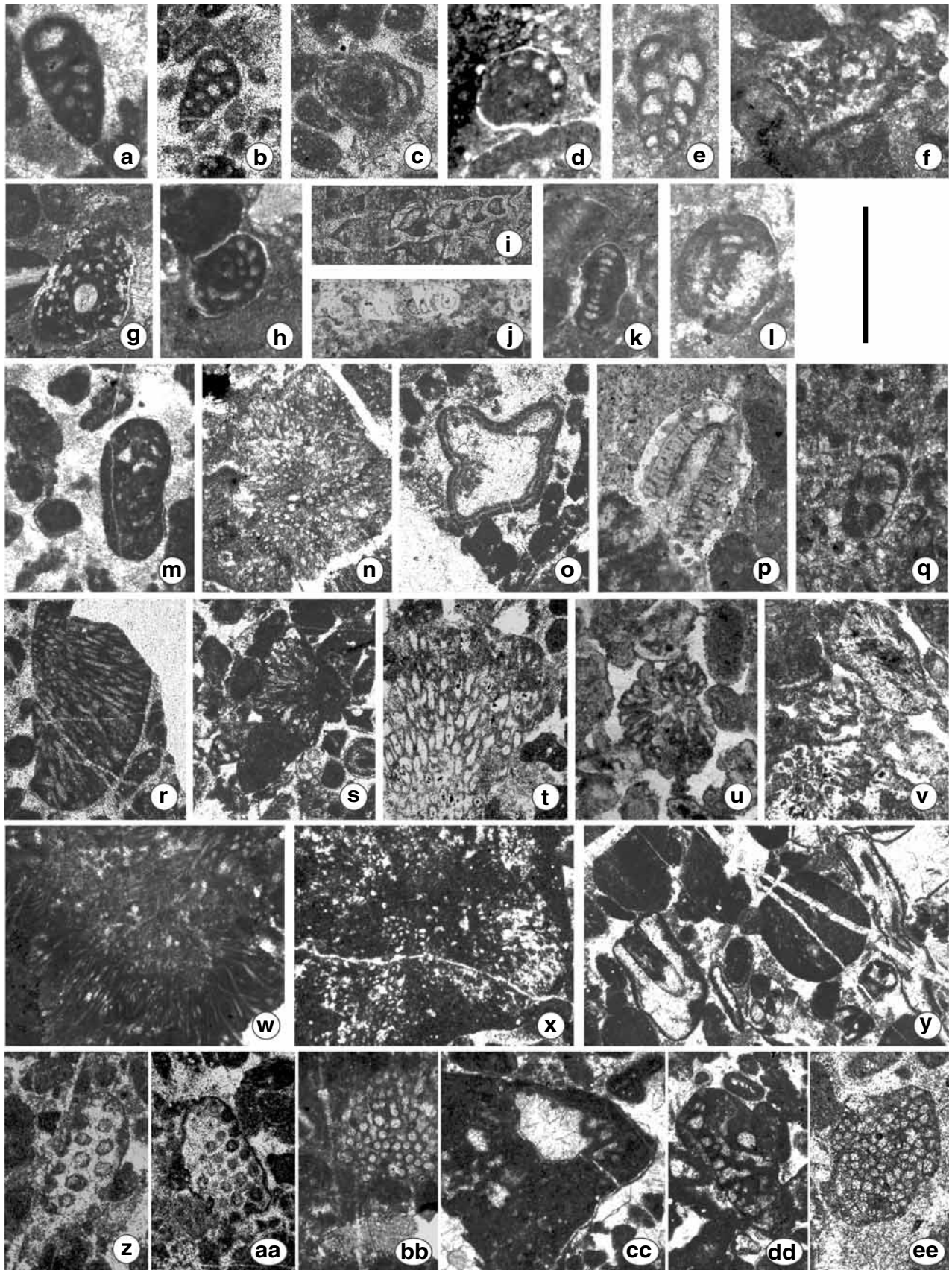


Fig. 9 **a–q** Characteristic microfossils from the interval 63–115 m (samples S26–45, T9–16) and figures **r–ee** from the interval 115–190 m (samples S46–70, T17–25). The scale bar is 500 μm , except figures **n–ee**, where it is 1250 μm . **a** *Textularia* sp., sample S30. **b** *Valvulina* sp., sample T13. **c** *Glomospira* sp., sample T9. **d** *Placopsilina* sp. sample S38. **e** *Siphovalvulina* gr. *variabilis*, sample S42. **f–g** *Orbitopsella primaeva*, samples S36 and S38. **h** *Bosniella croatica*, sample S38. **i** *Dentalina* sp., sample T11. **j** *Marginulina* sp., sample S33. **k** *Agerella martana*, sample S38. **l** *Involutina farinacciae*, sample S38. **m** *Everticyclammina* mg. *virguliana–praevirguliana*, sample S30. **n** Rivulariacean-like cyanobacteria, sample T12. **o** *Thaumatoporella parvovesiculifera*, sample T9. **p** dasycladalean alga, *Steinmanniporella?* sp., sample S38. **q** serpulid *Carpathiella triangulate*, sample S31. **r** *Rivularia lissaviensis*, samples T23. **s** *Rivularia piae*, sample T22. **t** *Rivularia* sp., sample T19. **u** *Hedstromieia* sp., sample S53. **v** *Arabicodium bicaezensis*, sample S53. **w** *Pseudogirvanella?* sp., sample S50. **x** *Solenopora?* sp., sample T19. **y** Dasycladacea spp., sample T24. **z** *Selliporella?* sp., sample T25. **aa** *Anisoporella* sp., sample T17. **bb** *Petrascula* sp., sample S55. **cc** *Pseudolithocodium carpathicum*, sample S49. **dd** *Bacinella irregularis*, sample T22. **ee** *Thaumatoporella parvovesiculifera*, sample T25

eupelagic sedimentary rocks. Evaluation of the microfossil assemblages led to the conclusion that the studied succession represents a long time-range from the Late Triassic to the Middle Jurassic.

Based on biostratigraphic constraints, the age of Unit 1 is latest Carnian to Rhaetian; taking into account the aspect of the interpretation of the depositional history of the succession, it is most probably Late Norian. The basal redeposited carbonate bed of this unit contains mixed shallow-marine (reefal) and deep-marine fossils. The toe-of-slope deposits grade upward into basinal carbonates.

The basinal carbonates are overlain by basinal fine-grained siliciclastics (Unit 2). This striking change in the lithology reflects enhanced terrigenous input, which was probably the result of a significant climate change (increased humidity). Although no age-diagnostic fossils were found in this unit, a Norian–Rhaetian age-assignment of the overlying Unit 3 suggests that it might be connected with the early Rhaetian Kössen Event (e.g., Berra et al. 2010). Siliciclasts of the sandstone beds were derived predominantly from low- to medium-grade metamorphic rocks. Consequently, Hercynian (or perhaps the pre-Hercynian) ranges may have been the provenance.

Gravity-induced carbonate deposits, akin to those found in the basal part of the section, resume above the siliciclastic unit (Unit 3). Based on the foraminiferal fauna, these beds are still Late Triassic, most probably late Rhaetian in age. The appearance of the toe-of-slope carbonate deposits above the basinal sandstones, shales, and marls suggest decreasing humidity and/or platform progradation.

The overlying cherty limestone (Unit 4), which is rich in radiolarians and sponge spicules, was formed in a relatively deep basin. Following the sea-level lowstand in the latest Triassic, the earliest Jurassic is characterized by rising sea

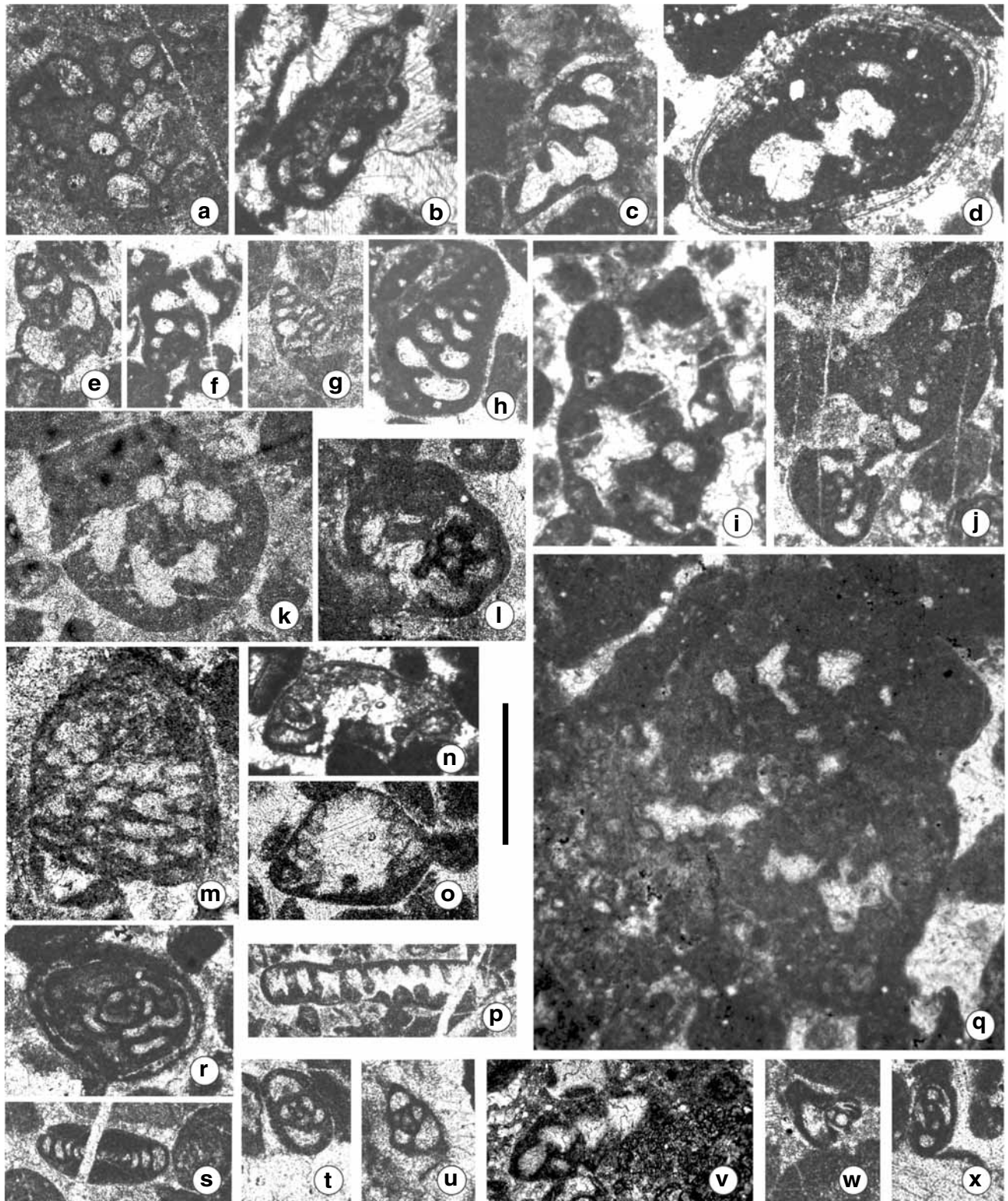
level (e.g., Hallam and Wignall 1999; Hallam 2001; Hesselbo et al. 2004). Accordingly, although no age-diagnostic fossils were encountered here, this striking sea-level rise probably happened in the earliest Jurassic (Hettangian).

In the next interval (Unit 5), which can be assigned to the late Sinemurian–early Pliensbachian, the silty, argillaceous, and siliceous basin facies are dominant, punctuated by thin carbonate intercalations containing redeposited shallow-marine fossil elements. The composition of the scarce siliciclastic material is similar to that in the deeper part of the section. Although in the Early Jurassic sedimentation took place in a relatively deep basin, the intercalations of gravity-induced, fine-grained carbonate deposits indicate the survival of shallow-marine carbonate factories in the neighborhood of the basin.

The next part of the succession (Unit 6) is made up predominantly of carbonates; basin and toe-of-slope facies alternate. Based on the foraminiferal fauna, it is assigned to the Bajocian–Bathonian. Compared to the previous one, the quantity, size, and composition of the siliciclastic material do not change in this interval, indicating relative continuity of the depositional system. However, the predominance of the carbonate lithology and the higher proportion of the redeposited beds suggest a sea-level highstand and related platform progradation.

In the higher part of the succession (Unit 7), carbonate lithoclasts of shallow-marine origin were observed in the redeposited carbonate beds, along with individual ooids, peloids, and bioclasts of shallow-marine biota (Middle Jurassic in age). Some of these sand-size clasts contain Upper Triassic and Lower Jurassic fossils. An actively producing carbonate factory must have been the source of the redeposited individual shallow-marine carbonate grains. The carbonate lithoclasts were derived from the erosion of Upper Triassic and Lower Jurassic rocks. In the uppermost carbonate gravity-flow beds, co-occurring mm-sized fragments of medium-grade metamorphic rocks and lithic components of an ophiolite complex were found, suggesting a remarkable change in the provenance.

Red siliceous shale and radiolarite occur in the topmost part of the measured section (Unit 8) and similar rock types continue upward along the valley. Based on lithological and microfacies characteristics, and considering the result of age determination (Late Bajocian to Early Bathonian), these rocks can be assigned to the Zlatar Formation, amended by Gawlick et al. (2017), referring to previous work of Djerić et al. (2007, 2010). Gawlick et al. (2017) noted that the original underlying rocks of this formation were not known in its type area in the DOB. In the Trijebinska Reka section, the underlying succession is exposed and the transition between redeposited toe-of-slope facies and the radiolarian-rich eupelagic basin facies is also visible.



Comparison with age-equivalent successions

Age-equivalent successions are known in the Krš Gradac area in the neighborhood (see Fig. 1c) of the studied section.

They are overthrust by the ophiolitic *mélange* (Gawlick et al. 2017), i.e., they have a structural position akin to that of the Trijebinska Reka section but they show a strikingly different development (see Gawlick et al. 2009, 2017).

Fig. 10 Characteristic microfossils from the interval 115–190 m (samples S46–70, T17–25). The scale bar is 500 μm , except figure a, where it is 1250 μm . **a** *Radiomura cautica*, sample T25. **b** *Placopsilina* sp., sample S49. **c** *Subbdellodina haeusleri*, sample S65. **d** *Tubiphytes* sp., sample T24. **e** *Siphovalvulina* gr. *variabilis*, sample T22. **f, g** *Riyadhella* mg. *praeregularis*—*regularis* samples T23 and T25. **h** *Redmondoides lugeoni* sample T23. **i** *Ammobaculites* sp., sample S59. **j** *Bosniella* mg. *croatica* (below) and *Nautiloculina circularis*, sample T25. **k** cf. *Pseudopfenderina butterlini*, sample T25. **l** *Evertyclammina* mg. *virguliana* – *praevirguliana*, sample T19. **m** *Kilianina blancheti*, sample T21. **n** *Trocholina conica*, sample T20. **o** *T. palastiniensis*, var. low-spined, sample T20. **p** *T. palastiniensis* var. high-spined, sample T25. **q** *Pseudocyclammina* mg. *maynci*—*lituus* sample S54. **r** *Meandrovoluta asiagoensis*, sample T24. **s** *Ophthalmidium concentricum*, sample T26. **t** *Labalina rawiensis* sample T21. **u** *L. costata*, sample T21. **v** nubecularid foraminifera, sample S46. **w** *Protopenneroplis striata*, sample T24. **x** *Archaeosepta* sp., sample T22

We must note that Upper Triassic (Carnian to Rhaetian) grey, thin-bedded cherty limestones with marl interlayers commonly occur as blocks in the ophiolitic mélange in other areas of the DOB. They typically exhibit radiolarian wackestone/packstone texture with scarce fragments of thin-shelled bivalves. Very fine grained turbiditic interbeds with shallow-marine debris also occur, but rarely. These successions representing predominantly hemipelagic basin facies were assigned to the amended Upper Triassic Grivska Formation by Gawlick et al. (2017) and Sudar and Gawlick (2018).

South of the DOB, in the Lim Subunit of the East Bosnian–Durmitor Unit (or East Bosnian–Durmitor Megaunit after Gawlick et al. 2017; see Fig. 1b), Lower and Middle Jurassic cherty limestones of basin facies were reported (Haas et al. 2011). In the Pre-Karst Unit and in the Bosnian Zone, Hercegovina and Montenegro, a thick succession (Vranduk Group) of alternating graded calcarenites (mostly oolites) and argillaceous micritic limestones and shales with radiolarite intercalations is known. It was formed during the Late Triassic (?) through the Jurassic to the earliest Cretaceous (e.g., Pamić et al. 1998; Dragičević and Velić 2002; Haas et al. 2011).

From the aspects of reconstruction of the paleogeographic setting and depositional conditions of the studied section, the age-equivalent sections of the Slovenian Basin are particularly important because, along with biostratigraphically well-constrained age-assignments, a number of detailed sedimentological studies were reported from that area (e.g., Rožič et al. 2009, 2013a; Kolar-Jurkovšek 2011; Gale et al. 2012, 2013, 2014). This deep basin came into existence between the Adriatic-Dinaridic Carbonate platform (ADCP) and the Julian Carbonate Platform (JCP) in the early Carnian and continued until the Early Cretaceous (Buser 1989; Vrabcet et al. 2009). The drowning of the JCP took place in the late Pliensbachian and then it was transformed into a submarine high (Rožič et al. 2017, 2018). Since the euphotic conditions did not change significantly on the ADCP, from

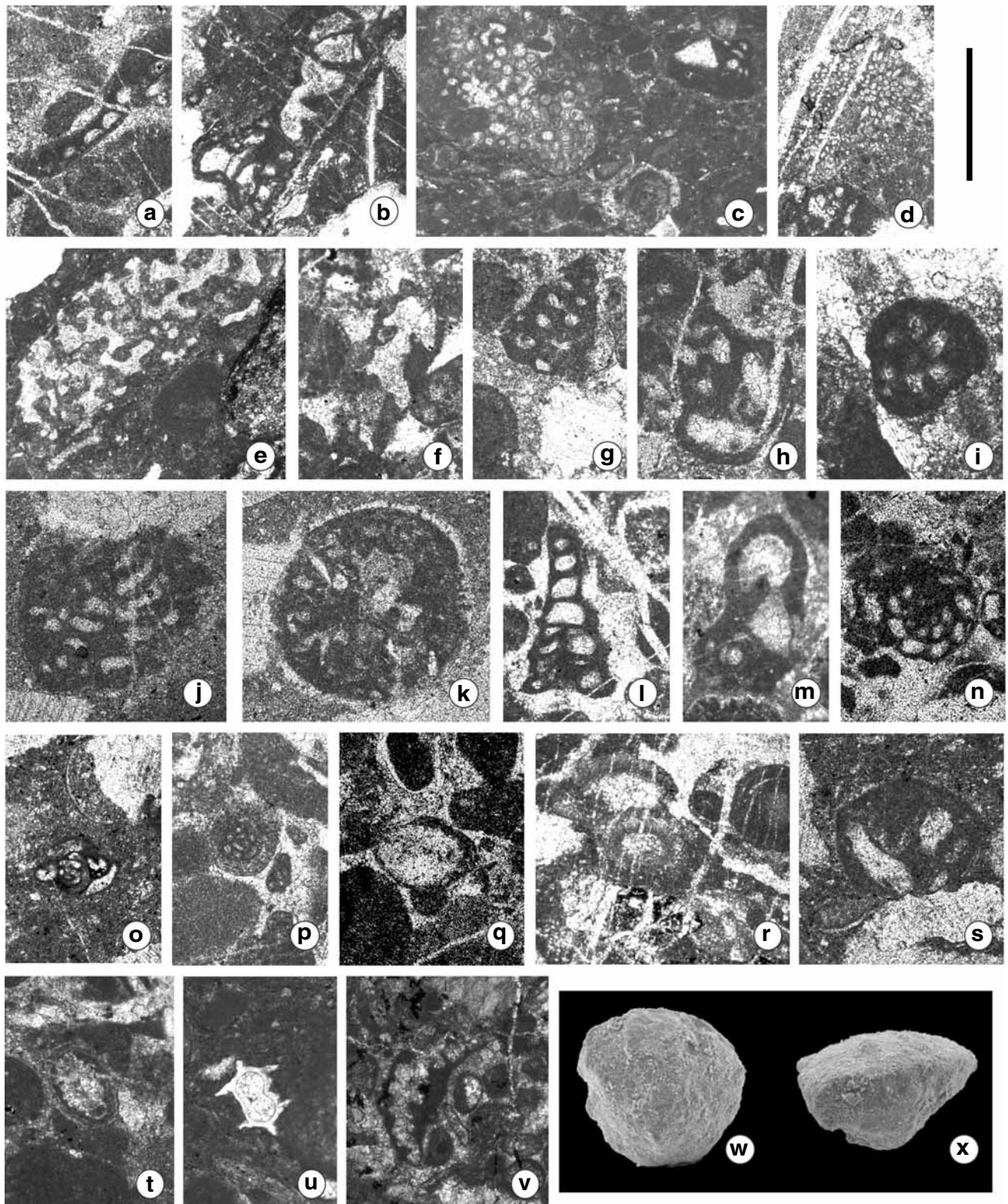
that time this platform may have been the only source of the redeposited shallow-marine carbonate grains. Accordingly, the Bajocian–Bathonian (?Callovia) limestone breccia (debrite) and graded oolitic, bioclastic limestone successions (Tolmin Formation) of toe-of-slope facies reported from the Slovenian Basin (Rožič and Popit 2006; Rožič et al. 2018) were derived from the ADCP. Similar Middle Jurassic redeposited lithoclastic and oolitic, bioclastic toe-of-slope facies were also described from the Croatian segment of the ADCP foreland (Dragičević and Velić 2002; Bucković et al. 2004).

Paleogeographic setting of the studied section

During the initial stages of the Alpine plate-tectonic cycle, the areas of the South Alpine–Outer Dinaridic–Outer Hellenidic ranges belonged to the Tethyan margin of the North African part of Gondwana, which was broken off from here, later forming the Adria microplate (e.g., Csontos and Vörös 2004; Berra and Angiolini 2014). The westward propagation of the Vardar branch of the Neotethys Ocean reached this domain in the Middle Triassic and led to the disintegration of the previously existing large carbonate ramps; smaller isolated carbonate platforms and interplatform basins were formed on the passive margin (e.g., Haas et al. 1995). As a result of the intense terrigenous influx, some of these basins were filled up and occupied by the extending platforms. However, renewal of the extensional tectonic movements in the early Carnian led to the development of a large basin system, which separated the huge ADCP from a series of smaller to larger isolated platforms (Fig. 13). Among them, the Upper Triassic deposits of the JCP are well preserved and excellently exposed. The JCP is separated from the ADCP by the Slovenian Basin. Records of similar Late Triassic platforms are known in the Sana-Una and Jadar Units from the Vardar Zone and the Drina–Ivanjica Unit in the Inner Dinarides, and most probably also in the Bükk Unit, North Hungary, that reached its present-day position as the result of large-scale Cenozoic displacements (e.g., Csontos and Vörös 2004, Kovács and Haas 2010). On the basis of this paleogeographic model, the block containing the Krš Gradac section could have originated from one of these platforms. The data on the foreslope deposits made possible the reconstruction of the ADCP slope toward the interplatform basin-system (Bosnian Basin), but only sporadic records on the internal basin succession are available. The section in the Trijebinska Reka valley representing a significant stratigraphic range is one of them, and that is why the inferences of its study are of particular importance.

Depositional model and provenance analysis

Since the carbonate platforms located along the oceanward belt of the passive margin (see Figs. 13, 14) were drowned



near the Triassic/Jurassic boundary and in the Early Jurassic, it is highly probable that the ADCP was the source of the platform-derived carbonate grains in the Middle Jurassic beds of the studied section, at least prior to the onset of

the active margin stage. The sand-sized carbonate grains of the Upper Triassic and Lower Jurassic sequences were probably derived from the ADCP as well. Determination of the provenance of siliciclastic material derived mostly

Fig. 11 Figures **a–u** characteristic microfossils from the interval 190–230 m (samples S6–12, T1–3) and figures **v–x** from the interval 230–239 m (samples S84–87, T29). For figures **a–e**, **r** and **v** scale bar is 1000 μm ; for figures **f–q** and **s–u** 500 μm , and for figures **w** and **x**, 350 μm . **a** *Pseudolithocodium carpathicum*, sample T26. **b** *Bacinella irregularis*, sample T28. **c** *Petrascula* sp. and *Planivolutina carinata*, sample S77. **d** *Solenopora?* sp., sample T28. **e** stromatoporoid, sample T28. **f** *Ammobaculites*, sample T26. **g** *Valvulina* sp., sample T26. **h** *Siphovulvulina* gr. *variabilis*, sample T28. **i** *Bosniella* mg. *croatica*, sample T26. **j**, **k** *Lituosepta recoanensis*, sample T28. **l** cf. *Kilianina blancheti*, initial part, sample T28. **m** *Everticyclammina* mg. *virguliana–praevirguliana*, sample S83. **n** *Nautiloculina circularis*, sample T26. **o**, **p** *Meandrovoluta asiagoensis*, sample T28. **q** *Involutina farinaciae*, sample T26. **r** agglutinated polychaetid *Terebella lapilloides*, sample T28. **s** *Variosotoma cohlea*, sample T28. **t** *Involutina liassica*, sample S74. **u** *Paralinvolutina* mg. *tenera*, sample S77. **v** *Alpinophragium perforatum*, sample S86; **w**, **x** *Duostomina turboidea*, sample T29, SEM images

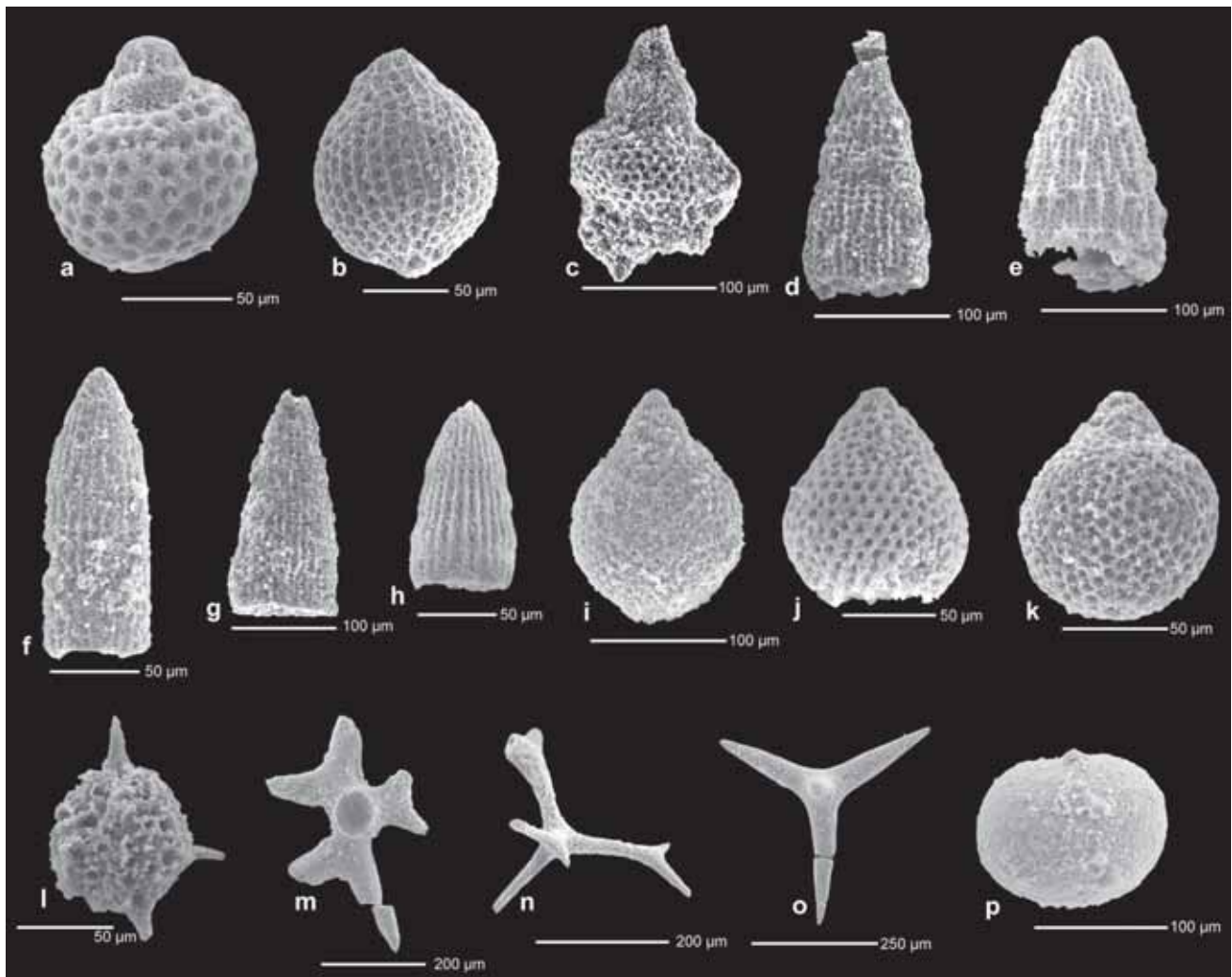


Fig. 12 Radiolarians and sponge spicules found in radiolarite (samples T29 and BG3). **a** *Zhamoidellum* cf. *ventricosum* Dumitrica, sample BR3. **b** *Striatojaponocapsa conexa* (Matsuoka) BR3. **c** *Eucyrtidiellum* cf. *quinatum* Takemura, sample T29. **d** *Parashuum carpathicum* Widz and DeWever, sample T29. **e** *Transhsuum maxwelli* (Pessagno), sample BR3. **f** *Archeodictyomitra prisca* Kozur and Mostler, sample T29. **g** *Archaeodictyomitra whalenae* Kozur and Mostler, sample T29. **h** *Archaeodictyomitra whalenae* Kozur and

Mostler, BR3. **i** *Praewilliriedellum convexum* (Yao), sample T29. **j** *Praewilliriedellum* cf. *robustum* (Matsuoka) sample BR3. **k** *Praewilliriedellum robustum* (Matsuoka) sample T29. **l** ?*Pantanellium* sp. indet, sample T29. **m–o** Various megascleres (sponge spicules) from sample T29. **p** Rhax (sponge spicule), sample T29. **m** Dichotriaene (Tetractine), sample T29. **n** Dichotriaene (Tetractine), sample T29. **o** Oxycalthrop (Tetractine), sample T29. **p** Rhax (Polyactine), sample T29

from low- and medium-grade metamorphic rocks is a more difficult question and requires the evaluation of the paleogeographic setting, and the analysis of various depositional models. During the passive-margin evolutionary stage from the Middle Triassic to the earlier part of the Middle Jurassic, only the Adriatic microplate may have been the source of the siliciclasts.

The relationship of carbonate platform evolution and terrigenous influx has been the subject of detailed investigations in the Southern Alps (Breda et al. 2009; Breda and Preto 2011; Dal Corso et al. 2015). In this region, the enhanced siliciclastic influx, as a result of the Carnian Pluvial Episode, led to drowning of most of the previously existing carbonate

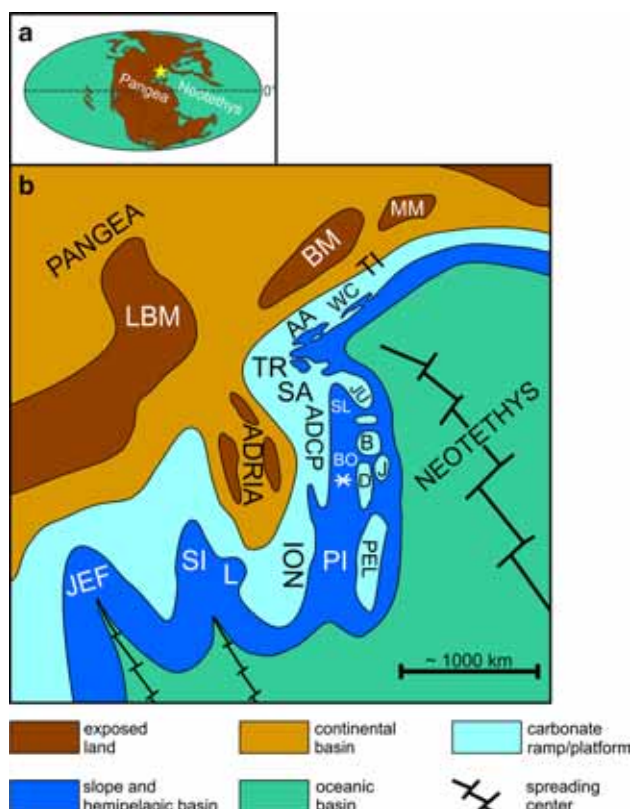


Fig. 13 Paleogeographic setting of the study area during the Late Triassic. **a** Position of the western Neotethys region. **b** Position of the study area (white star) within the western Neotethys region (the map is compiled after Dercourt et al. 1993; Haas et al. 1995, 2009; Szulz 2000; Schmid et al. 2008; Berra and Angiolini 2014). LBM London-Brabant Massif, BM Bohemian Massif, MM Malopolska Massif, AA Austroalpine Units, WC Central and Inner West Carpathian Units, TI Tisza Unit, TR Transdanubian Range, SL Slovenian basin, JU Julian Alps, B Bükk Unit, ADCP Adriatic Dinaridic Carbonate Platform, BO Bosnian Zone, D Drina-Ivanjica Unit, JA Jadar Block, SI Sicilian Basin, L Lagonegro Basin, JEF Jefra Basin, PI Pindos Basin, PEL Pelagonian-Subpelagonian Units

platforms and the filling of the interplatform basins with redeposited shallow-marine carbonates and terrigenous siliciclastic sediments. In the late Carnian lowstand period, a terrestrial to shallow-marine mixed siliciclastic-carbonate succession was formed under semi-arid conditions (Travenanses Formation). According to the paleoenvironmental interpretations there is a lateral transition and interfingering between the alluvial plain, flood basin, and the lagoonal-peritidal internal platform facies of the Dolomia Principale (Breda and Preto 2011). The drainage basin of the small ephemeral streams was southward, i.e., towards the internal part of the Adriatic microplate. Carnian bauxites were reported from the Outer Dinarides, which are covered by an upper Carnian carbonate-siliciclastic succession that overlain the Dolomia Principale (Celarc 2008; Dozet and Buser 2009). According to the Dolomia Principale facies

model of Caggiati et al. (2018), there is a near-continent siliciclastic mudflat behind the internal platform lagoon that is separated by the shelf crest from the gently sloping external platform progressing into the steeper foreslope. Outer-platform carbonate sands, together with slope material, were resedimented via turbidity currents and deposited on the slope apron. Fine carbonates together with minor siliciclastics derived from the mudflats were mostly distributed in the periplatform basin from suspensions of hypopycnal and mesopycnal flows. According to Caggiati et al. (2018) the overall depositional system of the Permian Guadalupian carbonate platform is remarkably similar to that of the Dolomia Principale/Dachstein platform. We basically agree with this statement; the comprehensive summary on the evolution of the Guadalupian platform by Kerans et al. (2013) demonstrated the modes and the controlling factors of bypassing of siliciclastic sediments through the carbonate platform to the slope and shedding into the basin. On the basis of the Guadalupian model, assuming channelized transport, the influx of a significant amount of siliciclastic sediment can also be explained. Taking into account the chronostratigraphic constraints, the deposition of the siliciclastic basin facies of the studied section (Unit 2) can be bound to the Rhaetian humid episode (Kössen Event).

The active margin evolution of the Neotethys Ocean began during the Middle Jurassic, probably in the Bajocian (Gawlick et al. 2017). This is manifested in the disruption of the external belts of the shelf and the development of a westward-propagating nappe stack and the obduction of the ophiolite nappes during the late Middle to Late Jurassic (Schmid et al. 2008; Gawlick et al. 2017). This significant change in the geodynamic setting of the region must be taken into account for the provenance analysis of the Bajocian-Bathonian redeposited sediments. Two options emerged for the interpretation of the results of our observations. According to the first one, the redeposited individual carbonate grains might have originated from those shallow-marine environments, which may have developed above the nappe stack (Fig. 14). The fragments of the Upper Triassic-Lower Jurassic carbonate rocks and the medium-grade metamorphic rocks were derived from the frontal part of the nappe stack, and the ophiolitic components from the overthrusting ophiolite nappes. These lithoclasts were transported first onto the shallow margin of the basin and then redeposited via gravity-driven flows into the deep internal basin. According to the second option, the geodynamic changes did not significantly influence the depositional processes and did not cause a fundamental change in the provenance of the redeposited grains. This means that the ADCP remained the source of the individual carbonate grains. Thus, the Upper Triassic-Lower Jurassic carbonate lithoclasts were derived from the high-angle erosional slope of the ADCP, and both the medium-grade metamorphic and the ophiolitic

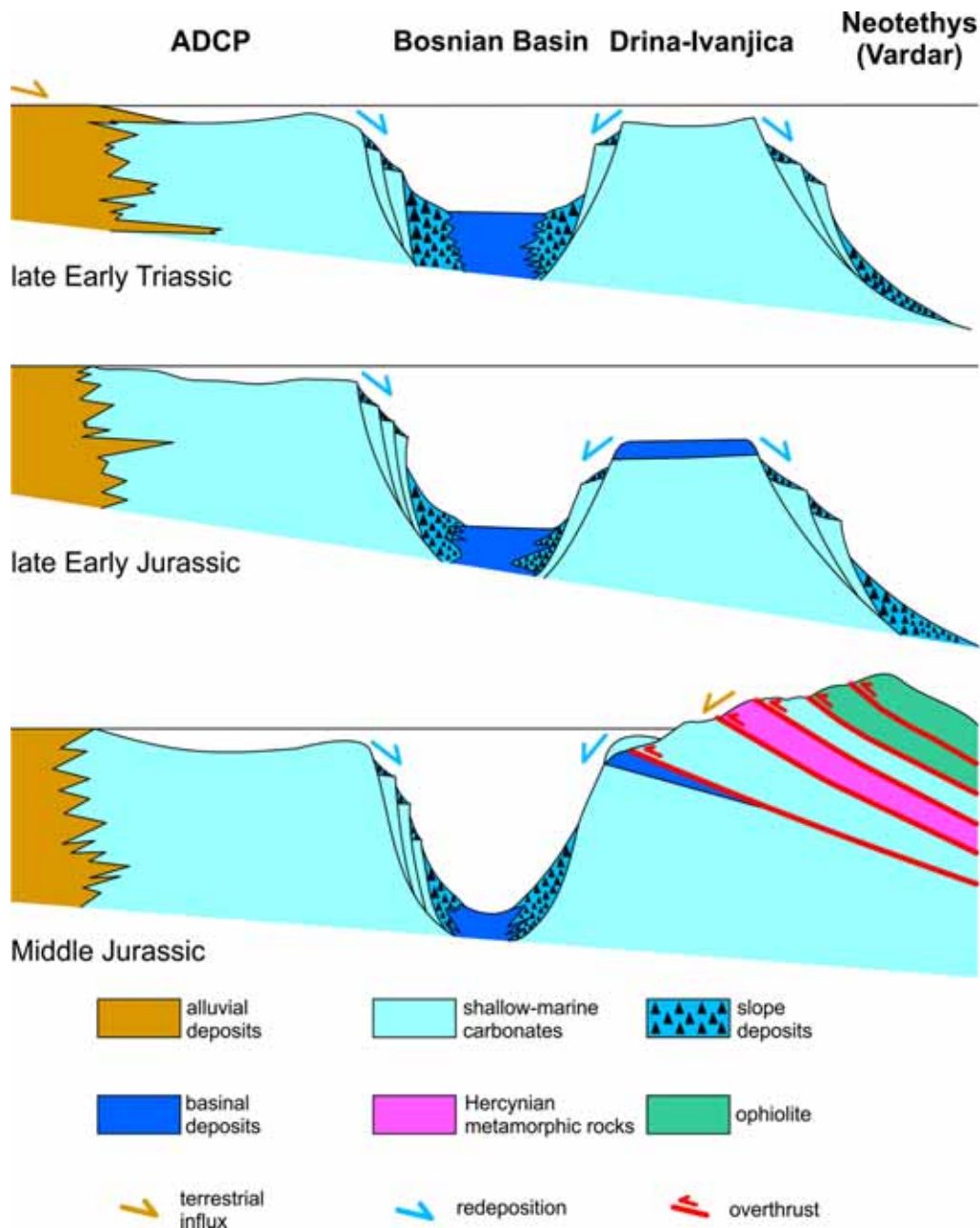


Fig. 14 Conceptual cross sections for demonstrating the structural evolution and related changes in sediment deposition on the southern margin of the western Neotethys, from the passive to the active stage

components were transported on to the platform from the Hercynian outcrops of the Adriatic microplate.

Conclusions

The results of our biostratigraphic studies suggest that along the eastern side of the Trijebinska Reka valley, an approximately 230-m-thick Upper Triassic to Middle Jurassic succession is exposed. It is made up mostly of carbonate rocks,

with intercalation of shale and fine siliciclastic sandstone beds representing toe-of-slope and pelagic basin facies. The fine-grained debris flow/grain flow and turbidity current deposits of the toe-of slope facies consist predominantly of carbonate grains (mostly bioclasts) derived from ambient carbonate platform/ramp environments. This means that during the long Late Triassic to Middle Jurassic time range of sediment deposition, active shallow-marine carbonate factories must have existed in the neighborhood of the depositional basin.

During the Late Triassic to Early Jurassic period, various amounts of fine siliciclasts, derived predominantly from low- to medium-grade metamorphic rocks, were transported into the basin, leading to the deposition of sandstone and shale bed-sets. A small amount of terrigenous siliciclasts are usually present also in the carbonate debrite/turbidite bed-sets. In the redeposited beds in the upper part of the Middle Jurassic succession, the co-occurrence of shallow-marine bioclasts, medium-grade metamorphic rocks, and lithic components of an ophiolite complex were encountered, suggesting multiple episodes of redeposition of components derived from various sources.

Evaluation of the paleogeographic reconstructions and the inferences of sedimentological studies performed in the Slovenian Basin and the age-equivalent sections along the foreslope ADCP led to the conclusion that the section in the Trijebinska Reka valley was probably located in the internal part of the Bosnian Basin. Our studies provide data on the depositional history of this basin and the provenance of the redeposited components.

Since the carbonate platforms, located along the oceanward belt of the passive margin, were drowned by the Early Jurassic, the ADCP should have been the source of the platform-derived carbonate grains in the Middle Jurassic beds of the studied section, at least prior to the onset of the active-margin stage. During the passive-margin evolutionary stage, from the Middle Triassic to the earlier part of the Middle Jurassic, only the Adriatic microplate should have been the source of the siliciclasts. Outer platform carbonate sands, containing generally only minor amounts of terrigenous siliciclasts, were subjected to resedimentation by turbidity currents. However, during the humid episodes a large amount of terrigenous material may have arrived into the deep basins via channelized transport. The chronostratigraphic constraints suggest that deposition of the siliciclastic basin facies found in the lower part of the studied section can be connected to the Rhaetian humid episode.

The active margin evolution of the Neotethys Ocean began during the Middle Jurassic and led to the disruption of the external belts of the shelf, the development of a westward-propagating nappe stack and the obduction of the ophiolite nappes. This significant change in the geodynamic setting of the region must be taken into consideration for the provenance analysis of the Bajocian–Bathonian redeposited sediments.

A significant lithofacies change was recorded in the uppermost part of the studied section, where the predominantly redeposited toe-of-slope facies progresses upward into a radiolarian-rich eupelagic basin facies. This change of facies probably occurred during the Early Bathonian.

The studied section records an approximately 50 Ma-long chapter from the history of the western Neotethys margin. Considering the paleogeographic reconstructions and the

analogies of age-equivalent sections, this slice may represent the development of the internal part of the Bosnian Basin, which was located between the ADCP and the Drina–Ivanjica Unit. In the DOB, and within it also in the neighborhood of the studied sections, other slices representing a similar age range but showing a strikingly different development, are known. Further systematic and detailed studies of these slices are required for the proper fitting of the jigsaw puzzle that may lead to the correct reconstruction of the paleogeographic setting and better understanding of the complex geodynamic history of this segment of the Neotethys Ocean.

Acknowledgements Open access funding provided by Eötvös Loránd University (ELTE). This paper is the result of the work on the project “Comparative study of the geological evolution of the Dinarides and the Pannonian region” from 2008 to 2015 that was performed within the framework of co-operation between the Serbian Academy of Sciences and Arts (Project F-22) and the Hungarian Academy of Sciences. The work was supported by the Hungarian National Research Found, Grant No. K 113013, the Hantken Foundation. This is MTA-MTM-ELTE Paleo Contribution No. 268. The research of M.N. Sudar and D. Jovanović was also supported by the Ministry of Education, Science and Technical Development of the Republic of Serbia (ON 176015). The authors are indebted to the editor-in-chief Maurice Tucker and the reviewers Hans-Jürgen Gawlick and Špela Goričan for their very valuable notes and suggestions. We also express our thanks for the linguistic corrections by Henry Lieberman.

Open Access This article is distributed under the terms of the Creative Commons Attribution 4.0 International License (<http://creativecommons.org/licenses/by/4.0/>), which permits unrestricted use, distribution, and reproduction in any medium, provided you give appropriate credit to the original author(s) and the source, provide a link to the Creative Commons license, and indicate if changes were made.

References

- Ampferer O, Hammer W (1918) Erster Bericht über eine 1918 im Auftrage und auf Kosten der Akademie der Wissenschaften ausgeführte geologische Forschungsreise in Westserbien. Sitzungsber Kaiserliche Akad Wiss Wien, Math-Naturw Kl, Abt I 127(H. 8-9):635–668
- Bernecker M (2005) Late Triassic reefs from the Northwest and South Tethys: distribution, setting, and biotic composition. *Facies* 51:442–453. <https://doi.org/10.1007/s10347-005-0067-4>
- Berra F, Angiolini L (2014) The evolution of the Tethys region throughout the Phanerozoic: a brief tectonic reconstruction. In: Marlow L, Kendall C, Yose L (eds) *Petroleum systems of the Tethyan region*. AAPG Mem, Tulsa, pp 1–27
- Berra F, Jadoul F, Anelli A (2010) Environmental control on the end of the Dolomia Principale/Hauptdolomit depositional system in the central Alps: coupling sea-level and climate changes. *Palaeogeogr Palaeoclimatol Palaeoecol* 290:138–150. <https://doi.org/10.1016/j.palaeo.2009.06.037>
- Bortolotti V, Chiari M, Kodra A, Marcucci M, Marroni M, Mustafa F, Prella M, Pandolfi L, Principi G, Saccani E (2006) Triassic MORB magmatism in the Southern Mirdita Zone (Albania). *Ofioliti* 31(1):1–9. <https://doi.org/10.4454/ofioliti.v31i1.323>
- Breda A, Preto N (2011) Anatomy of an Upper Triassic continental to marginal-marine system: the mixed siliciclastic-carbonate

- Travenanzes Formation (Dolomites, northern Italy). *Sedimentology* 58:1613–1647
- Breda A, Preto N, Roghi G, Furin S, Meneguolo R, Ragazzi E, Fedele P, Gianolla P (2009) The Carnian Pluvial Event in the Tofane area (Cortina d'Ampezzo, Dolomites, Italy). *Geo Alp* 6:80–115
- Bucković D, Tešović BC, Gušić I (2004) Late Jurassic paleoenvironmental evolution of the Western Dinarides (Croatia). *Geol Carpath* 55(1):3–18
- Buser S (1989) Development of the Dinaric and the Julian carbonate platforms and of the intermediate Slovenian Basin. *Mem Soc Geol It* 40(1987):313–320
- Caggiati M, Gianolla P, Breda A, Celarc B, Preto N (2018) The start-up of the Dolomia Principale/Hauptdolomit carbonate platform (Upper Triassic) in the eastern Southern Alps. *Sedimentology* 65:1097–1131. <https://doi.org/10.1111/sed.12416>
- Celarc B (2008) Carnian bauxite horizon on the Kopitov grič near Borovnica (Slovenia) – is there a “forgotten” stratigraphic gap in its footwall? *Geologija* 51(2):147–152. <https://doi.org/10.5474/geologija.2008.015>
- Chiari M, Djerić N, Garfagnoli F, Hrvatović H, Krstić M, Levi N, Malasoma A, Marroni M, Menna F, Nirta G, Pandolfi L, Principi G, Sacconi E, Stojadinović U, Trivić B (2011) The geology of the Zlatibor-Maljen area (western Serbia): a geotraverse across the ophiolites of the Dinaric-Hellenic collisional belt. *Ofoliti* 36(2):139–166. <https://doi.org/10.4454/OFIOLITI.V36.I2.3>
- Csontos L, Vörös A (2004) Mesozoic plate tectonic reconstruction of the Carpathian region. *Palaeogeogr Palaeoclimatol Palaeoecol* 210:1–56
- Dal Corso J, Gianolla P, Robert J, Newton RJ, Franceschi M, Roghi G, Caggiati M, Raucsik B, Budai T, Haas J, Preto N (2015) Carbon isotope records reveal synchronicity between carbon cycle perturbation and the “Carnian Pluvial Event” in the Tethys realm (Late Triassic). *Global Planet Change* 127:79–90
- Dercourt J, LE Ricou, Vrielynck B (eds) (1993) Atlas Tethys palaeoenvironmental maps and explanatory notes. 1–307, maps 1–14. (Gauthier-Villars), Paris
- Dimitrijević MD (1997) Geology of Yugoslavia. Geological Institute Gemini, Spec publ:1–187, Belgrade
- Dimitrijević MN, Dimitrijević MD (1973) Olistostrome Mélange in the Yugoslavian Dinarides and Late Mesozoic Plate Tectonics. *J Geol* 81(3):328–340
- Dimitrijević MN, Dimitrijević MD (1979) The Olistostrome, Polyphase and Recycled Ophiolite Mélange. Zbornik radova, IV godišnji znanstveni skup Sekcije za primjenu geologije, geofizike i geokemije Znanstvenog savjeta za naftu JAZU (Stubičke Toplice, 9-12.5.1978), JAZU, Radovi Znanstvenog savjeta za naftu, Sekcije za primjenu geologije, geofizike i geokemije Znanstvenog savjeta za naftu (Zagreb). Ser. A, knj. 7:101–117 (in **Serbo-Croatian, English summary**)
- Dimitrijević MD (1991) Triassic carbonate platform of the Drina–Ivanjica element (Dinarides). *Acta Geol Hung* 34(1-2):15–44
- Dimitrijević MN, Dimitrijević MD, Karamata S, Sudar M, Gerzina N, Kovács S, Dosztály L, Gulácsi Z, Pelikán P, Gy Less (2003) Olistostrome/mélanges—an overview of the problems and preliminary comparison of such formations in Yugoslavia and Hungary. *Slovak Geol Mag* 9(1):3–21
- Djerić N (2002) Jurassic Radiolarians of the Dinaridic Ophiolite Belt between Nova Varoš and Sjenica (SW Serbia). Master thesis, Faculty Mining and Geology, University of Belgrade, pp 1–80 (in Serbian, English Abstract)
- Djerić N, Gerzina N, Schmid S (2007) Age of the Jurassic radiolarian chert formation from the Zlatar Mountain (SW Serbia). *Ofoliti* 32(2):101–108
- Djerić N, Gerzina N, Simić D (2010) Middle Jurassic radiolarian assemblages from Zlatar Mt. (SW Serbia). *Geol an Balk poluos* 71:119–125
- Dozet S, Buser S (2009) Triassic. In: Pleničar M, Ogorelec B, Novak M (eds) *The geology of Slovenia*. Geološki zavod Slovenije, Ljubljana, pp 161–214
- Dragičević I, Velić I (2002) The northeastern margin of the Adriatic Carbonate Platform. *Geol Croat* 55:185–232
- Gale L, Kolar-Jurkovič T, Šmuc A, Rožič B (2012) Integrated Rhaetian foraminiferal and conodont biostratigraphy from the Slovenian Basin. *Eastern Southern Alps. Swiss J Geosci* 105(3):435–462
- Gale L, Kastelic A, Rožič B (2013) Taphonomic features of Late Triassic foraminifera from Mount Begunjščica, Karavanke Mountains. *Slovenia. Palaios* 28(11):771–792. <https://doi.org/10.2110/palo.2014.102>
- Gale L, Rožič B, Mencin E, Kolar-Jurkovič T (2014) First evidence for Late Norian progradation of Julian Platform towards Slovenian Basin, Eastern Southern Alps. *Riv. It Paleontol Stratigr* 120:191–214
- Gawlick HJ, Sudar M, Đerić N, Jovanović D, Lein R, Missoni S, Suzuki H (2007) Late Middle Jurassic radiolarians from the ophiolitic-radiolaritic mélange of the Dinaridic Ophiolite Belt. 8th Workshop on Alpine Geological Studies (Davos, Switzerland, 10.–12. October 2007), Abstract volume (poster): pp 25–26
- Gawlick HJ, Frisch W, Hoxha L, Dumitrică P, Krystyn L, Lein R, Missoni S, Schlagintweit F (2008) Mirdita Zone ophiolites and associated sediments in Albania reveal Neotethys Ocean origin. *Int J Earth Sci (Geol Rundsh)* 97:865–881. <https://doi.org/10.1007/s00531-007-0193-z>
- Gawlick HJ, Sudar M, Suzuki H, Djerić N, Missoni S, Lein R, Jovanović D (2009) Upper Triassic and Middle Jurassic radiolarians from the ophiolite mélange of the Dinaridic Ophiolite Belt, SW Serbia. *N Jb Geol Paläontol Abh* 253(2-3):293–311. <https://doi.org/10.1127/0077-7749/2009/0253-0293>
- Gawlick HJ, Missoni S, Suzuki H, Sudar M, Lein R, Jovanović D (2016) Triassic radiolarite and carbonate components from a Jurassic ophiolitic mélange (Dinaridic Ophiolite Belt). *Swiss J Geosci* 109(3):473–494. <https://doi.org/10.1007/s00015-016-0232-5>
- Gawlick HJ, Sudar M, Missoni S, Suzuki H, Lein R, Jovanović D (2017) Triassic-Jurassic geodynamic history of the Dinaridic Ophiolite Belt (Inner Dinarides, SW Serbia). *J Alp Geol* 55:1–167
- Haas J, Kovács S, Krystyn L, Lein R (1995) Significance of Late Permian-Triassic facies zones in terrane reconstructions in the Alpine-North Pannonian domain. *Tectonophysics* 242:19–40
- Haas J, Pomoni-Papaioannou F, Kostoulou V (2009) Comparison of the Late Triassic carbonate platform evolution and Lofer cyclicity in the Transdanubian Range, Hungary and Pelagonian Zone, Greece. *Central Eur Geol* 52:153–184
- Haas J, Kovács S, Gawlick HJ, Grădinaru E, Karamata S, Sudar M, Cs Péro, Mello J, Polák M, Ogorelec B, Buser S (2011) Jurassic Evolution of the Tectonostratigraphic Units of the Circum-Pannonian Region. *Jb Geol B-A* 151(34):281–354
- Hallam A (2001) A review of the broad pattern of Jurassic sea-level changes and their possible causes in the light of current knowledge. *Palaeogeogr Palaeoclimatol Palaeoecol* 167:23–37
- Hallam A, Wignall PB (1999) Mass extinctions and sea-level changes. *Earth Sci Rev* 48:217–250. [https://doi.org/10.1016/s0012-8252\(99\)00055-0](https://doi.org/10.1016/s0012-8252(99)00055-0)
- Hammer W. (1923) II. Die Diabashornsteinschichten. In: Ampferer O, Hammer W, Ergebnisse der geologischen Forschungsreise in Westserbien. *Denkschr Akad Wiss, Math-natw K1* 98 (Sitzung vom 21 April 1921): pp 45–56
- Hesselbo et al (2004) Hesselbo SP, Robinson SA, Surlyk F (2004) Sea-level change and facies development across potential

- Triassic-Jurassic boundary horizons, SW Britain. *J Geol Soc London* 161:365–379
- Jones G, Robertson AHF (1991) Tectono-stratigraphy and evolution of the Mesozoic Pindos Ophiolite and related units, northwestern Greece. *J Geol Soc London* 148:267–288
- Jovanović O, Novković M, Čanović M (1979) Litho-bio-facial characteristics of Diabase-chert formation on the Sjenica region. *Zb rad, IV god znan skup Sek prim geol, geofiz geokem Znan sav naftu (Stubičke Toplice, 9–12. 5.1978), Znan sav naftu JAZU, Sek prim geol, geofiz geokem Zagreb, Ser A 7:147–154 (in Serbo-Croatian, English summary)*
- Jovanović D, Ljubović—Obradović D, Radovanović Z (1994) Bedded limestones like separate member of Diabase—Chert Formation (Brajaska reka, SW Serbia). *Vesnik, (Geozavod, Beograd) Ser A, B 46:145–153 (in English, Serbian summary)*
- Karamata S (2006) The geological development of the Balkan Peninsula related to the approach, collision and compression of Gondwanan and Eurasian units. In: Robertson AHF, Mountrakis D (eds) *Tectonic development of the eastern Mediterranean region. Geol Soc Spec Publ London* 260:155–178
- Karamata S, Dimitrijević MN, Dimitrijević MD (1999) Oceanic realms in the central part of the Balkan Peninsula during the Mesozoic. *Slovak Geol Mag* 5:173–177
- Karamata S, Dimitrijević MD, Dimitrijević MN, Milovanović D (2000) A correlation of ophiolitic belts and oceanic realms of the Vardar Zone and the Dinarides. In: Karamata S, Janković S (eds) *Proc Int Sym “Geology and Metallogeny of the Dinarides and the Vardar Zone” (Zvornik, 3–6 October, 2000), Acad Sci Arts Rep Srpska, Coll Monogr, 1, Dep Nat, Math Tech Sci 1:191–194, Banja Luka, Sarajevo*
- Kerans Ch, Playton TE, Phelps R, Scott SZ (2013) Ramp to rimmed shelf transition in the Guadalupian (Permian) of the Guadalupe Mountains, West Texas and New Mexico. In: Verwer K, Playton TE, Harris PM (eds) *Deposits, Architecture, and Controls of Carbonate Margin, Slope, and Basinal Settings, vol 105. SEPM Spec Publ, Tulsa, pp 26–49*
- Kilias A, Frisch W, Avgerinas A, Dunkl I, Falalakis G, Gawlick HJ (2010) Alpine architecture and kinematics of deformation of the northern Pelagonian nappe pile in the Hellenides. *Austrian J Earth Sci* 103(1):4–28
- Kilias A, Thomaidou E, Falalakis G, Avgerinas S, Sfeikos A, Katrivanos M, Vamvaka A, Fassoulas Ch, Pipera K (2016) A geological cross-section through northern Greece from the Pindos to Rhodope Mountains: a field trip guide across the External and Internal Hellenides. In: Kilias A, Lozios S (eds) *Geological field trips in the Hellenides. J Virtual Explor* 50:1–108. <https://doi.org/10.3809/jvirtex.2016.08685>
- Kolar-Jurkovšek T (2011) Latest Triassic conodonts of the Slovenian Basin and some remarks on their evolution. *Geologija* 54(1):81–90
- Kovács S, Haas J (2010) Displaced South Alpine and Dinaridic elements in the Mid-Hungarian Zone. *Cent Eur Geol* 53:135–164
- Kovács S, Sudar M, Gradinaru E, Gawlick HJ, Karamata S, Haas J, Cs Péró, Gaetani M, Mello J, Polák M, Aljinović D, Ogorelec B, Kolar-Jurkovšek T, Jurkovšek B, Buser S (2011) Triassic Evolution of the Tectonostratigraphic Units of the Circum-Pannonian Region. *J Geol B-A* 151(3+4):199–280
- Missoni S, Gawlick HJ, Sudar MN, Jovanović D, Lein R (2012) Onset and demise of the Wetterstein Carbonate Platform in the mélange areas of the Zlatibor Mountain (Sirogojno, SW Serbia). *Facies* 58(1):95–111. <https://doi.org/10.1007/s10347-011-0274-0>
- Ozsvárt P, Dosztály L, Migiros G, Tselepidis V, Kovács S (2012) New radiolarian biostratigraphic age constraints on Middle Triassic basalts and radiolarites from the inner Hellenides (northern Pindos and Othrys Mountains, northern Greece). *Int J Earth Sci* 101(6):1487–1501. <https://doi.org/10.1007/s00531-010-0628-9>
- Pamić J, Gušić I, Jelaska V (1998) Geodynamic evolution of the Central Dinarides. *Tectonophysics* 297:251–268
- Pessagno EA, Newport RL (1972) A technique for extracting Radiolaria from radiolarian cherts. *Micropaleontology* 18:231–234. <https://doi.org/10.2307/1484997>
- Radoičić R, Jovanović D, Sudar M (2009) Stratigraphy of the Krš Gradac section (SW Serbia). *Geol Balk poluos* 70:23–41. <https://doi.org/10.2298/GABP0970023R>
- Radovanović Z, Ljubović—Obradović D, Jovanović D (1996) Bedded limestones of Trijebinska reka (Sjenica, SW Serbia). In: Vasić N (ed) *VII skup sedimentologa Jugoslavije (Beograd, 3–5. 6. 1996), Apstrakti, Savez geol druš Jugoslavije, Kom sedimentol, Rud-geol fak Beograd, Inst MKPG, Lab. sedimentol, 42–43, 80, Beograd (in Serbian and English)*
- Radovanović Z, Nastić V, Popević A (2004) Geological map of the Republic of Serbia, Prijepolje 2, 1:50,000. *Dir Environ Prot, Republic of Serbia, Belgrade, Min Sci Environ Prot*
- Rožič B (2009) Perbla and Tolmin formations: revised Toarcian to Tithonian stratigraphy of the Tolmin Basin (NW Slovenia) and regional correlations. *Bull Soc Géol France* 180:411–430
- Rožič B, Popit T (2006) Redeposited limestones in the Middle and Upper Jurassic successions of Slovenian basin. *Geologija* 49(2):219–234
- Rožič B, Gerčar D, Oprčkal P, Švara A, Turnšek D, Kolar-Jurkovšek T, Udovč J, Kunst L, Fabjan T, Popit T, Gale L (2018) Middle Jurassic limestone megabreccia from the southern margin of the Slovenian Basin. *Swiss J Geosci. https://doi.org/10.1007/s00015-018-0320-9*
- Rožič B, Gale L, Fabjan T, Šmuc A, Kolar-Jurkovšek T, Čosović V, Turnšek K (2013a) Problematika južnega obrobja slovenskega bazena na primeru razvoja ponikvanske tektonske krpe. *Geol Z* 22:138–143
- Rožič B, Gale L, Kolar-Jurkovšek T (2013b) Extent of the Upper Norian – Rhaetian Slatnik formation in the Tolmin Nappe, eastern Southern Alps. *Geologija* 66(2):175–186
- Rožič B, Kolar-Jurkovšek T, Žvaba Rožič P, Gale L (2017) Sedimentary record of subsidence pulse at the Triassic/Jurassic boundary interval in the Slovenian Basin (eastern Southern Alps). *Geol Carpath* 68(6):543–561. <https://doi.org/10.1515/geoca-2017-0036>
- Schefer S, Egli D, Missoni S, Bernoulli D, Fügenschuh B, Gawlick HJ, Jovanović D, Krystyn L, Lein R, Schmid S, Sudar M (2010) Triassic metasediments in the Internal Dinarides (Kopaonik area, southern Serbia): stratigraphy, paleogeography and tectonic significance. *Geol Carpath* 61(2):89–109. <https://doi.org/10.2478/v10096-010-0003-6>
- Schlagintweit F, Velić I (2011) New and poorly known Middle Jurassic larger benthic foraminifera from the Karst Dinarides of Croatia. *Geol Croat* 64(2):81–100. <https://doi.org/10.4154/gc.2011.08>
- Schmid SM, Bernoulli D, Fügenschuh B, Matenco L, Schefer S, Schuster R, Tischler M, Ustaszewski K (2008) The Alpine-Carpathian-Dinaride-oregenic system: correlation and evolution of tectonic units. *Swiss J Geosci* 101:139–183
- Senowbari-Daryan B (2016) Upper Triassic miliolids of “Cucurbita group”: aspects of the systematic classification. *Jahrb Geol B-A* 156:187–215
- Sudar MN, Gawlick HJ (2018) Emendation of the Grivska Formation in their type area (Dinaridic Ophiolite Belt, SW Serbia). *Geol Balk poluos* 79(1):1–19. <https://doi.org/10.2298/GABP1879001S>
- Sudar MN, Gawlick HJ, Lein R, Missoni S, Kovács S, Jovanović D (2013) Depositional environment, age and facies of the Middle Triassic Bulog and Rid formations in the Inner Dinarides (Zlatibor Mountain, SW Serbia): evidence for the Anisian break-up of the Neotethys Ocean. *N Jahrb Geol Paläontol Abh* 269(3):291–320. <https://doi.org/10.1127/0077-7749/2013/0352>

- Szulz J (2000) Middle Triassic evolution of the northern Peri-Tethys area as influenced by early opening of the Tethys Ocean. *Ann Soc Geol Pol* 70:1–48
- Toljić M, Matenco L, Ducea MN, Stojadinović U, Milivojević J, Djerić N (2013) The evolution of a key segment in the Europe-Adria collision: the Fruška Gora of northern Serbia. *Glob Planet Change* 103:39–62. <https://doi.org/10.1016/j.gloplacha.2012.10.009>
- Vishnevskaya VS, Djerić N, Zakariadze GS (2009) New data on Mesozoic Radiolaria of Serbia and Bosnia, and implications for the age and evolution of oceanic volcanic rocks in the Central and Northern Balkans. *Lithos* 108:72–105. <https://doi.org/10.1016/j.lithos.2008.10.015>
- Vrabec M, Šmuc A, Pleničar M, Buser S (2009) Geological evolution of Slovenia—An overview. In: Pleničar M, Ogorelec B, Novak M (eds) *The geology of Slovenia*. Geološki zavod Slovenije, Ljubljana, pp 23–40
- Živaljević M, Mirković M, Ćirić A (1983) *Basic Geological Map of SFRY, 1:100,000, Sheet Bijelo Polje (K 34-28)*, Sav geol zavod, Beograd (Zavod geol istraž SRG-Titograd, Geozavod-OOOR Geološki institut, Beograd, 1965–1977)